

**CASE FILE
COPY**

NASA MEMO 12-26-58A

NASA MEMO 12-26-58A

NASA

*W-012
300-019*

MEMORANDUM

THE EFFECT OF LEADING-EDGE SWEEP AND SURFACE INCLINATION
ON THE HYPERSONIC FLOW FIELD OVER A BLUNT FLAT PLATE

By Marcus O. Creager

Ames Research Center
Moffett Field, Calif.

**NATIONAL AERONAUTICS AND
SPACE ADMINISTRATION**

WASHINGTON

January 1959



NATIONAL AERONAUTICS AND SPACE ADMINISTRATION

MEMORANDUM 12-26-58A

THE EFFECT OF LEADING-EDGE SWEEP AND SURFACE INCLINATION

ON THE HYPERSONIC FLOW FIELD OVER A BLUNT FLAT PLATE

By Marcus O. Creager

SUMMARY

An investigation of the effects of variation of leading-edge sweep and surface inclination on the flow over blunt flat plates was conducted at Mach numbers of 4 and 5.7 at free-stream Reynolds numbers per inch of 6,600 and 20,000, respectively. Surface pressures were measured on a flat plate blunted by a semicylindrical leading edge over a range of sweep angles from 0° to 60° and a range of surface inclinations from -10° to $+10^\circ$.

The surface pressures were predicted within an average error of ± 8 percent by a combination of blast-wave and boundary-layer theory extended herein to include effects of sweep and surface inclination. This combination applied equally well to similar data of other investigations.

The local Reynolds number per inch was found to be lower than the free-stream Reynolds number per inch. The reduction in local Reynolds number was mitigated by increasing the sweep of the leading edge.

Boundary-layer thickness and shock-wave shape were changed little by the sweep of the leading edge.

INTRODUCTION

A major portion of the trajectory of hypersonic winged vehicles may be in the upper reaches of the atmosphere where flow occurs at low unit Reynolds numbers. Thus, appreciable boundary-layer growth may occur over wings and control surfaces of a hypersonic vehicle. The leading edges of these surfaces may be or become sufficiently blunt to produce detached bow shock waves. Both the boundary-layer growth and bow-shock-wave strength affect local pressures in the flow field over these surfaces. In addition, these two effects may be altered by angle of attack and by sweep of the leading edge of the airfoil.

Theoretical analysis of these real flows is difficult because these two effects, boundary-layer growth and bow-shock-wave detachment, occur simultaneously. However, these effects have been treated separately, and the important parameters have been pointed out. The theoretical analysis by Lees and Probstein (ref. 1) and Lees (ref. 2) of the case of an ideally sharp plate in viscous hypersonic flow indicated there is a parameter, $M^3/\sqrt{\text{Re}_x}$, which predicts the magnitude of the pressure rise brought about by boundary-layer growth in the absence of detached bow shock waves. In order to assess the effect of the blunt leading edge on the inviscid flow field, Lees and Kubota (ref. 3) and Cheng and Pallone (ref. 4) utilized the blast-wave theory of Taylor (ref. 5) and Sakurai (ref. 6). Their analogy to this problem pointed out that the blast wave parameter was useful in prediction of surface pressure where boundary-layer growth might be unimportant. In the case of real flows, either wind tunnel or flight, the effects of both the boundary-layer growth and the bow shock wave are present and must be considered together. A method for calculation of the high surface pressures obtained in these real flows over unswept and noninclined flat plates was outlined in reference 7. This method consists of a linear combination of the parameters pointed out by the viscous and inviscid theories mentioned above.

Strengthening of the bow shock wave due to leading-edge blunting was found in reference 7 to alter the local total pressures at the boundary-layer edge for some test conditions. This effect of blunting was also measured in experiments reported in references 8 and 9. Quantitative values of local total pressure are necessary to the calculation of local Mach number or local Reynolds number along the boundary-layer edge.

The general purpose of the research described in this paper was to study the effect of leading-edge sweep and angle of attack on the hypersonic flow field over blunt flat plates. In particular, it was hoped that the experimental data would verify an extension presented herein of the methods of reference 7 to include variation of angle of leading-edge sweep and angle of attack.

Experimental pressure-distribution data were obtained from blunt flat plates at angle of sweep and angle of attack in a rarefied gas stream. The results are compared with the results of other similar investigations.

SYMBOLS

- A empirical constant, $\frac{1}{\sqrt{C_w}}$ (See eq. (1).)
- b $\gamma \left[\frac{0.865}{M^2} \frac{T_w}{T} + 0.166(\gamma-1) \right]$ (See eq. (1).)

B	empirical constant, $\left(\frac{1}{2}\right)^{2/3}$ (See eq. (1).)
c	factor $c_\gamma(C_D)^{2/3}$ (See eq. (1).)
c_γ	constant, 0.112 for $\gamma = 1.4$; 0.169 for $\gamma = 1.67$ (See eq. (1).)
C_D	leading-edge pressure drag coefficient based on projected frontal area
C_w	constant of proportionality in the linear viscosity and temperature relation $\frac{\mu}{\mu_w} = C_w \left(\frac{T}{T_w}\right)$
d	diameter or thickness
D	pressure drag force on the semicylindrical leading edge
I	blast-wave pressure parameter, $\frac{M_\infty^2}{(s/d)^{2/3}}$
K	constant in equation (3)
M	Mach number
p	pressure
R	height of point on shock wave, see sketches (a) and (b)
Re	Reynolds number
s	coordinate in free-stream direction, see sketch (c)
T	temperature
u	velocity
x	coordinate length normal to leading edge, defined in sketch (c)
α	angle of attack, deg
γ	ratio of specific heats
Δ	bow-shock-wave detachment distance
δ	boundary-layer thickness

Ω	angle of sweep, deg
ω	exponent of viscosity-temperature relation defined by $\mu \sim T^\omega$
μ	viscosity
ρ	density
$\bar{\chi}$	interaction parameter, $\frac{M^3 \sqrt{C_w}}{\sqrt{Re_x}}$

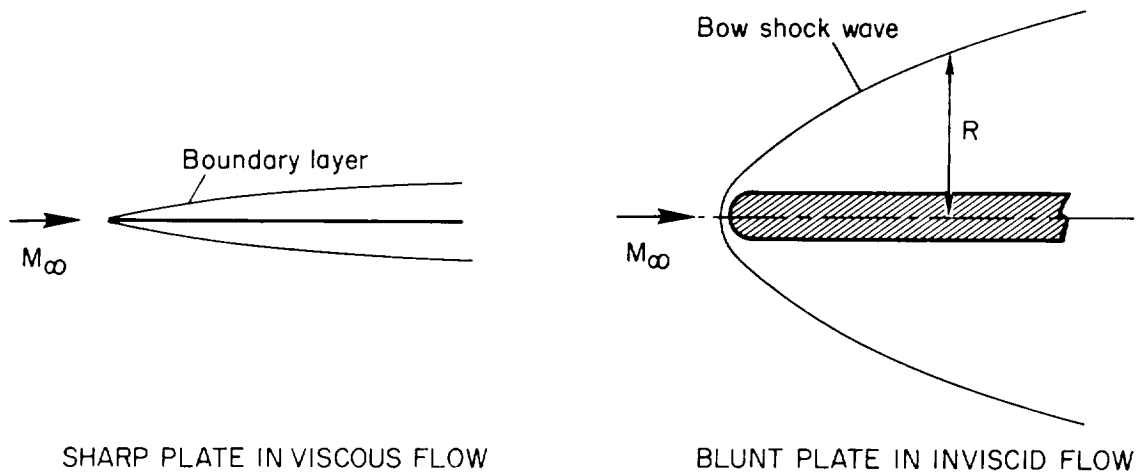
Subscripts

s	characteristic length for quantity along s coordinate direction
w	quantity based on body wall or surface conditions
x	characteristic length for quantity along x coordinate direction
α	quantity based on inviscid wedge condition far back on body
δ	quantity based on conditions at the boundary-layer edge
t_∞	total quantity based on undisturbed free-stream conditions
t_2	total quantity behind normal shock wave
t_δ	local total quantity at the boundary-layer edge
∞	quantity based on undisturbed free-stream conditions

ANALYSIS

Basic Method for Unswept Plates at Zero Angle of Attack

The results of reference 7 have indicated that a method based upon a combination of two simple theoretical flow models is adequate to evaluate some of the phenomena occurring over noninclined, unswept, flat plates. These two models are shown in sketch (a).



Sketch (a)

The left part of sketch (a) represents an ideally sharp plate in hypersonic viscous flow. The viscous effects near the surface of the sharp plate cause a growth of the boundary layer along the plate. The boundary-layer growth on this plate induces a rise in the static pressures at the plate surface. This theoretical flow model has been considered in detail by Lees and Probstein (ref. 1) and Lees (ref. 2). They have shown theoretically that the pressure increase due to the viscous effect is proportional to $M_\infty^3/\sqrt{\text{Re}_{\infty x}}$.

The right part of sketch (a) represents a blunt plate placed in inviscid hypersonic gas flow. The blunt leading edge introduces energy into the flow in the same manner as a moving explosion. This inviscid effect of the blunt leading edge causes a pressure rise at the plate surface. A detached bow shock wave forms ahead of the leading edge. This wave may remain highly curved far out into the flow field. These effects have been treated by Lees and Kubota (ref. 3) and Cheng and Pallone (ref. 4) in analogy to the theory of the blast wave (refs. 5 and 6). They showed the surface pressure rise produced by the blunt leading edge to be proportional to $C_D^{2/3} M_\infty^2 / (x/d)^{2/3}$ for two-dimensional flat plates.

In order to describe phenomena occurring over blunt plates in hypersonic viscous flow of real fluids, a combination of the two results obtained from the above-mentioned theoretical flow models was used in reference 7. The results obtained using this method indicate that the surface pressure, boundary-layer thickness, and shock-wave shape for unswept noninclined plates can be calculated, to good accuracy, in terms of free-stream properties. In addition, reference 7 shows that the

viscous and inviscid contributions to surface pressures can be linearly combined, and that the boundary-layer thickness prescribed by the viscous theory for sharp plates is not appreciably affected by blunting of the leading edge.

The surface pressures were found to be well predicted by the following linear combination of pressure terms obtained from the two theoretical flow models:

$$p/p_{\infty} = 1 + Ab_{\infty}\bar{x}_{\infty} + BcI \quad (1)$$

where

$$\bar{x}_{\infty} = \frac{M_{\infty}^3 \sqrt{C_W}}{\sqrt{Re_{\infty X}}}$$

$$I = \frac{M_{\infty}^2}{\left(\frac{x}{d}\right)^{2/3}}$$

and

$$b_{\infty} = \gamma \left[\frac{0.865}{M_{\infty}^2} \frac{T_W}{T_{\infty}} + 0.166(\gamma-1) \right]$$

$$c = c_{\gamma} (C_D)^{2/3}$$

$$A = \frac{1}{\sqrt{C_W}}$$

$$B = \left(\frac{1}{2}\right)^{2/3}$$

The constant c_{γ} is given in reference 4 as 0.112 for air and 0.169 for helium, and C_W is the proportionality constant in the linear viscosity relation $\mu/\mu_W = C_W(T/T_W)$.

The boundary-layer thickness was predicted by the results of viscous theory for the infinitely sharp plate as

$$\frac{\delta}{d} = \left[\frac{1.73}{M_{\infty}^2} \frac{T_W}{T_{\infty}} + 0.332(\gamma-1) + \frac{4.27}{M_{\infty}^2} \right] \frac{M_{\infty}^2 \sqrt{C_W}}{\sqrt{Re_{\infty d}}} \sqrt{\frac{x}{d}} \quad (2)$$

The shape of the shock wave produced by the blunt leading edge was found to be predicted by the results of the blast-wave analogy as

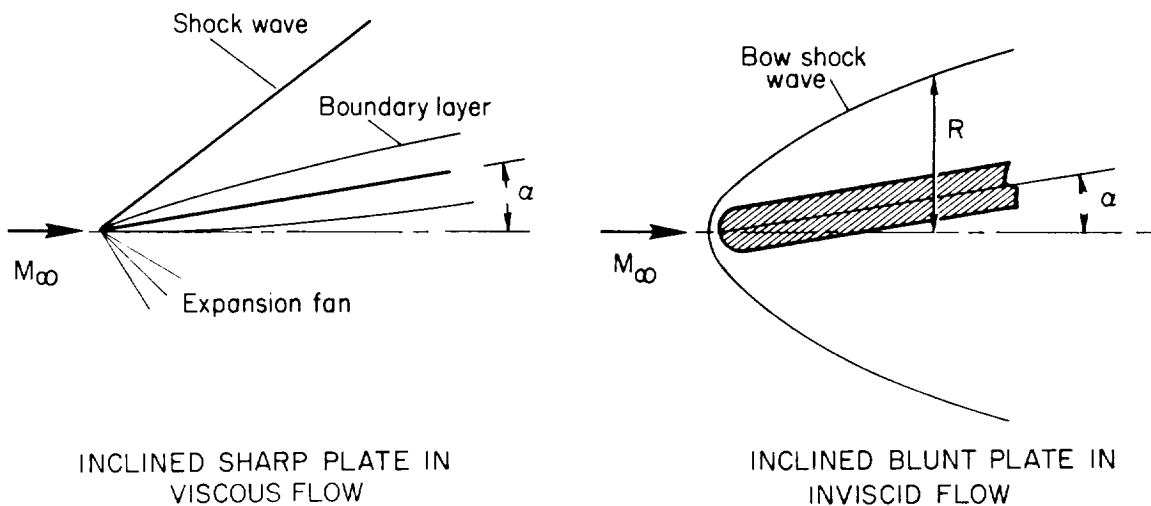
$$\frac{R}{d} = K(C_D)^{1/3} \left(\frac{x}{d}\right)^{2/3} \quad (3)$$

In reference 7 the value of K was found to be 1.45. The detached bow shock wave results in a reduction in the local total pressure along the boundary-layer edge. This effect has been found to persist as far back on bodies as measurements have been made.

With these results for unswept noninclined plates in mind, the effects of inclining the flat plates to the oncoming stream and of sweeping the leading edge will be considered next. The terms of the equations for surface pressure, shock-wave shape, boundary-layer thickness, and local total pressure will then be investigated for factors dependent on sweep and inclination. The variation of leading-edge sweep will be assumed to affect the blast-wave pressure increment, the shock-wave shape, and the local total pressure. The variation of surface inclination will be assumed to affect the viscous pressure increment and the boundary-layer thickness. The method and the assumptions involved will be assessed by use of the available experimental information.

Method for Angle of Attack

The two basic theoretical flow models used to describe the effects of surface inclination on the flow field are shown below in sketch (b).



Sketch (b)

The analysis of the hypersonic viscous flow over sharp flat plates (ref. 1) is applicable to inclined plates (shown on the left side of sketch (b)), provided the flow is considered to develop in the sharp-wedge inviscid flow field as determined either from oblique shock-wave or Prandtl-Meyer relations. Thus, the variables in the hypersonic interaction parameter, $\bar{\alpha}$, will be calculated from these sharp-nose inviscid flow properties that are assumed to exist far downstream on the inclined plate. The viscous contribution to the pressure on inclined surfaces can now be written for this more general case in the same form as before (see eq. (1)) except that the reference conditions are inviscid sharp wedge or " α conditions:"

$$Ab_{\alpha}\bar{\alpha}_{\alpha} = A\gamma \left[\frac{0.865}{M_{\alpha}^2} \frac{T_w}{T_{\alpha}} + 0.166(\gamma-1) \right] \frac{M_{\alpha}^3 \sqrt{C_w}}{\sqrt{Re_{\alpha x}}} \quad (4)$$

The inviscid flow over an inclined blunt plate is also shown in sketch (b). If the inviscid flow field is dominated by the blunt leading edge, the blast-wave analogy to the inviscid flow may be considered, to a first approximation, to depend only on leading-edge drag. Since small variation in angle of attack will not change the flow field about the leading edge appreciably, surface inclination will be assumed to have no effect on the drag of the leading edge; thus the shock wave will remain unaltered. Consequently, the inviscid pressure term, BcI , of equation (1) will not be changed by small variation in angle of attack.

If one assumes again that the viscous and inviscid contributions to the surface pressure are independent and can be linearly added, the surface pressures can then be calculated approximately by

$$\frac{p}{p_{\alpha}} = 1 + Ab_{\alpha}\bar{\alpha}_{\alpha} + \frac{p_{\infty}}{p_{\alpha}} \frac{BcM_{\infty}^2}{\left(\frac{x}{d}\right)^{2/3}} \quad (5)$$

The various blast-wave theories give the pressure behind the shock wave in ratio to the undisturbed pressure. Therefore, the ratio (p_{∞}/p_{α}) is introduced with the blast-wave pressure term in order to obtain the proper limiting condition of inviscid sharp-wedge pressure.

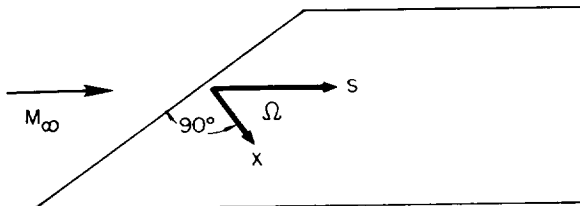
The boundary layer that develops along the inclined surface aft of a sharp leading edge, as in sketch (b), can be calculated from viscous compressible flow theory (ref. 1). The flow, however, is considered to develop in the inviscid sharp-wedge flow field, as previously stated. The boundary-layer thickness may be expressed for sharp inclined plates by:

$$\frac{\delta}{d} = \left[\frac{1.73}{M_\alpha^2} \frac{T_w}{T_\alpha} + 0.332(\gamma-1) + \frac{4.27}{M_\alpha^2} \right] \frac{M_\alpha^2 \sqrt{C_w}}{\sqrt{Re_{\alpha d}}} \sqrt{\frac{x}{d}} \quad (6)$$

In equation (6), the subscript α indicates that the quantity involved is calculated from inviscid sharp-wedge conditions.

Method for Leading-Edge Sweep

The two theoretical models of flow past the sharp and blunt bodies (sketch (a)) are again utilized to describe the effects of leading-edge sweep on the hypersonic viscous flow over noninclined blunt plates. The flow will be viewed in a plane which is normal to the plate surface and which contains the free-stream direction line s , sketch (c). For a sharp leading-edge plate the boundary-layer growth in the prescribed plane, should proceed approximately as given by equation (2) regardless of leading-edge sweep. Therefore, the pressure rise caused by the boundary-layer growth will be assumed to be unaffected by sweep.



Sketch (c)

The blunt plate with a swept leading edge in inviscid flow is considered next. If the assumption is retained that the leading edge dominates the inviscid flow field over the blunt flow model, it is only necessary to evaluate the variation of the leading-edge drag with leading-edge sweep. It is shown in reference 10 that if a detached shock exists at the leading edge, and the independence hypothesis of sweepback theory holds true, the variation of the leading-edge drag, measured in the free-stream direction, with sweep can be expressed in coefficient form as:

$$C_{D_s} = C_D \cos^3 \Omega \quad (7)$$

It is the leading-edge drag, D_s , acting in the free-stream direction that represents the energy fed into the transverse flow field over the blunt plate with swept leading edge. The blast wave or inviscid pressure term may then be obtained for swept plates from equations (1) and (7):

$$BcI = Bc_\gamma C_D^{2/3} \frac{M_\infty^2 \cos^2 \Omega}{(s/d)^{2/3}} \quad (8)$$

The resulting pressure increments contributed by the two theoretical flow models are now added in a linear combination as before. Thus, for a blunt plate with leading-edge sweep, the surface pressures are given by:

$$\frac{p}{p_{\infty}} = 1 + Ab_{\infty} \bar{x}_{\infty} + Bc \frac{M_{\infty}^2 \cos^2 \Omega}{(s/d)^{2/3}} \quad (9)$$

The equation of the shock-wave shape for a swept blunt plate may be obtained by combining equations (3) and (7) as

$$\frac{R}{d} = KC_D^{1/3} \left(\frac{s}{d} \right)^{2/3} \cos \Omega \quad (10)$$

Method for a Combination of Sweep and Angle of Attack

As before, if the viscous and blast-wave effects are assumed to be independent, the surface pressures can be calculated for the general case of an inclined plate with a swept blunt leading edge by the following equation:

$$\frac{p}{p_{\alpha}} = 1 + Ab_{\alpha} \bar{x}_{\alpha} + \frac{p_{\infty}}{p_{\alpha}} Bc \frac{M_{\infty}^2}{(s/d)^{2/3}} \cos^2 \Omega \quad (11)$$

where

$$Ab_{\alpha} \bar{x}_{\alpha} = A\gamma \left[\frac{0.865}{M_{\alpha}^2} \frac{T_w}{T_{\alpha}} + 0.166(\gamma-1) \right] \frac{M_{\alpha}^3 \sqrt{C_w}}{\sqrt{Re_{\alpha s}}}$$

Likewise the boundary-layer thickness for the blunt inclined plate is assumed not to be altered by sweep of the blunt leading edge. Therefore, the boundary-layer thickness may be calculated by:

$$\frac{\delta}{d} = \left[\frac{1.73}{M_{\alpha}^2} \frac{T_w}{T_{\alpha}} + 0.332(\gamma-1) + \frac{4.27}{M_{\alpha}^2} \right] \frac{M_{\alpha}^2 \sqrt{C_w}}{\sqrt{Re_{\alpha d}}} \sqrt{\frac{s}{d}} \quad (12)$$

The shock-wave shape is given approximately by equation (10) where R is measured to a zero angle of attack center line as noted in sketch (b).

Local Total Pressure Variation With Sweep

The presence of a detached bow shock wave has been shown (refs. 7, 8, and 9) to affect the local total pressure along the edge of the boundary layer on blunt flat plates. The local total pressure was found in some cases for unswept plates (ref. 7) to be reduced to that value of total pressure existing behind the bow shock wave and to remain reduced over the test length. Because of this reduction in local total pressure, values of local Reynolds numbers, Re_x , will be lower than free-stream Reynolds number, Re_{∞} . Therefore, to assess the possible variation of local total pressure with sweep of the leading edge, the following considerations are presented. The detached bow shock wave occurring ahead of and parallel to the blunt swept leading edge of the plate is now considered as a shock wave oblique to the free-stream flow. The ratio of total pressures across this wave can be obtained from shock-wave theory. The total pressure calculated behind this oblique wave is assumed to be equal to the local total pressure along the boundary-layer edge. Thus, for air:

$$\frac{P_{t\delta}}{P_{t\infty}} = \left(\frac{6M_{\infty}^2 \cos^2 \Omega}{M_{\infty}^2 \cos^2 \Omega + 5} \right)^{7/2} \left(\frac{6}{7M_{\infty}^2 \cos^2 \Omega - 1} \right)^{5/2} \quad (13)$$

where

$$M_{\infty} \cos \Omega > 1$$

It is conceivable that some distance back from the leading edge, the effect of the strong bow shock wave may diminish and the local total pressure may approach the free-stream value. However, measurement of this type of variation of local total pressure with distance back from the leading edge has not been reported in the literature. Therefore, the assumption is made here that $P_{t\delta}$ does not vary with distance from the nose. It is also assumed that the strength of the bow shock wave is not appreciably altered by small variation in angle of attack; therefore, inclination effects will not be considered here.

Calculation of Local Reynolds Numbers

Heat-transfer and skin-friction correlations have been successful when based on the local Reynolds numbers calculated from properties at the boundary-layer edge. (Accurate prediction of transition may also be dependent on knowledge of true local conditions of flow.) Therefore, the effect of blunting and boundary-layer growth on these local Reynolds numbers will be assessed and a method of calculation outlined.

The ratio of the local (unit) Reynolds number to the free-stream (unit) Reynolds number may be calculated from the definitions of these quantities as:

$$\frac{Re_x}{Re_{\infty x}} = \frac{M}{M_{\infty}} \frac{p}{p_{\infty}} \frac{\mu_{\infty}}{\mu} \sqrt{\frac{T_{\infty}}{T}} \quad (14)$$

The blunt leading edge and the boundary-layer growth affect local properties on which the ratios of equation (14) are dependent through the static-pressure rise and the total-pressure reduction. In reference 7 the isentropic relations were utilized locally at the boundary-layer edge to obtain the major dependence of the ratios of equation (14) on the total and static pressure. Thus, the Reynolds number ratio becomes:

$$\frac{Re_s}{Re_{\infty s}} = \left(\frac{p_{t\delta}}{p_{t\infty}} \right)^{\zeta} \left(\frac{p}{p_{\infty}} \right)^{1-\zeta} \sqrt{\frac{1-(T/T_t)}{1-(T_{\infty}/T_t)}} \quad (15)$$

where

$$\zeta \equiv (1+\omega) \left(\frac{\gamma-1}{\gamma} \right)$$

With the inviscid wedge values as the reference flow field, the Reynolds number ratio of equation (15) for plates at angle of attack becomes:

$$\frac{Re_s}{Re_{\alpha s}} = \left(\frac{p_{t\delta}}{p_{t\alpha}} \right)^{\zeta} \left(\frac{p}{p_{\alpha}} \right)^{1-\zeta} \sqrt{\frac{1-(T/T_t)}{1-(T_{\alpha}/T_t)}} \quad (16)$$

One effect of blunting is the possible reduction in local total pressure. This effect tends to reduce the local Reynolds number (see eq. (15) or (16)). In addition, the blunting causes a surface pressure rise which, by equation (16), may be seen to increase the local Reynolds number. These effects tend to oppose each other, and the effect which predominates depends on specific conditions. Blunting also alters the local temperatures on which the exponent ζ depends. The growth of the boundary layer produces a rise in pressure which, when considered alone in equation (15) or (14), increases the Reynolds number. The range of validity of equation (16) is a subject for experimental investigation.

TEST EQUIPMENT

Wind Tunnel and Nozzle

The tests were performed in the 8-inch low-density wind tunnel which has been described briefly in reference 7 and is shown schematically in figure 1. The variation of Mach number is accomplished by change of nozzles. The nozzles were designed as described in reference 7, wherein the nozzle operation at Mach number 4 was discussed. The Mach number 6 nozzle was calibrated at a stream static pressure of approximately 250 microns Hg absolute. The calibration of the stream was made by means of an impact pressure probe. With the assumption that the stream was isentropic the Mach numbers were calculated from the impact pressure readings by two methods. One method involves total pressure upstream of the nozzle; the other method involves the static pressures as measured 2 inches upstream of the nozzle exit plane. The agreement of the two methods may be noted in figure 2(a), wherein the results of an axial survey are shown. In figure 2(b), the results of a radial survey at a stream test station 3.5 inches from the nozzle exit plane are shown. The pertinent information concerning the air stream is tabulated in table I.

Models and Test Method

Four slab pressure models were fabricated from flat brass stock to a final thickness of 1/4 inch. The semicylindrical leading edges were swept to 0°, 30°, 45°, and 60°. The models were 4 inches wide which was sufficient to span the stream. The orifice chord line length was 7-1/2 inches for the swept models. Pressure orifices of 0.030-inch diameter were installed in the manner shown in figure 3(a). The angle of inclination of the surface to the stream was varied mechanically.

The pressure orifices were connected to a multiple-tube manometer. The working fluid of the manometer was a low-vapor-pressure vacuum-diffusion-pump oil. The manometer was mounted within the test chamber in order to shorten pressure lines. The reference leg was vented to the free-stream static pressure. The oil height differences were measured by means of a cathetometer (magnifying telescope) outside the test chamber.

An open-end type impact pressure probe was used for the flow field surveys. The probe was constructed of stainless-steel tubing flattened to an oval shape of 0.006 inch in height and 0.020 inch in width. The impact pressures sensed by this probe were indicated by an oil manometer. This probe was mounted to a traversing mechanism for motion along and across the jet. In addition, the probe could be rotated about an axis passing through the probe tip normal to the plate surface.

All impact surveys were obtained with the probe alined in the free-stream direction. Thus, in order to assess the possible errors in boundary-layer measurements due to local stream-angle variations with sweep, the probe was rotated through a range of angles of $\pm 20^\circ$ when placed at the edge of the boundary layer measured over the 30° swept model. The measured pressures showed that the probe was relatively insensitive to rotation of about 10° to 15° . The results indicated that the local stream velocity angles were within the flat portion of the probe curve and, therefore, accurate definition of stream direction was neither necessary nor possible. A simple analysis presented in appendix A indicates that the local stream angle would probably maximize at a value of 6.5° for conditions where the leading edge is swept to about 45° . Therefore, all data were obtained with the probe alined in the free-stream direction.

Near the leading edge of the plates the boundary layer was disturbed by the presence of the probe for these tests. Surveys were performed during the present tests in which the ratio of boundary-layer thickness to probe thickness was varied from 3.5 to 10 by increasing probe size. The probe size was found not to affect the measured thickness of boundary layer for the range of ratios mentioned above. The data for s/d of 1 to 1.5 were obtained for a probe to boundary-layer thickness ratio of about 2, and thus may be in error because of probe size effects. The remaining bulk of the data was obtained for values of this ratio greater than 3 and is thus not affected by probe size.

The pressure models were placed in the air stream so that the line of pressure orifices was coincident with the stream span center line. The leading-edge stagnation point of the orifice chord line was placed on the axis of the stream at a distance of 3.5 inches from the Mach number 6 nozzle exit plane for all conditions of sweep and inclination. The impact pressure probe was moved, during a survey, normal to the plate surface. Such surveys were obtained at various locations along the pressure orifice line.

The pressure model (fig. 3(b)) tested in the Mach number 4 stream was blunted by a semicylinder of 1/2-inch diameter. This model was described in reference 7. Surface pressures were measured at various angles of attack; however, no flow-field surveys were obtained over this model.

The thin leading-edge models were constructed by attaching a 0.002-inch-thick strip of gage stock to the upper surface of the unswept model and of the 60° sweep model. The thin leading edge was extended to about 1/4 inch ahead of the blunt nose of the test body, see figure 3(c).

Spanwise pressure measurements were obtained at 0° and 10° angle of attack by moving the model orifice chord line off the stream span center line. These measurements were made in order to assess jet boundary effects.

The range of tests conducted in this investigation is summarized in table II.

RESULTS AND DISCUSSION

In the analysis section it was assumed that the various contributions were independent and could be added linearly to obtain a simple method of calculating surface pressures on flat plates. The available experimental surface static-pressure data extending over a wide range of variables will be utilized in the assessment of this method. Experimental results of shock-wave shape and boundary-layer thickness measurements are also presented in substantiation of the assumptions involved in the independence and superposition of the viscous and inviscid flow field. These experimental results were obtained from impact pressure surveys of the flow field over the flat plates for various conditions of the leading-edge sweep, angle of attack and leading-edge bluntness.

Surface Pressures

The surface pressures were measured over a range of angles of attack, angles of leading-edge sweep, Mach numbers, and Reynolds numbers. The effects of sweep and angle of attack will be shown separately, and then in correlated form. In figure 4, the measured surface pressures in ratio to free-stream pressure are presented as a function of distance measured in the s direction (see sketch (c)) from the leading edge for several angles of sweep. It may be noted that the pressures are high near the leading edge and decrease with distance from the leading edge. Also, from figure 4, it may be noted that the surface pressures decrease as the sweep of the leading edge is increased.

The surface pressures measured on inclined plates whose leading edges were unswept are shown in figure 5 for Mach number 4 and figure 6 for Mach number 5.7. The pressures are noted to decrease with increase in distance from the leading edge. The ratio of surface pressure to inviscid wedge pressure may be seen from figure 5 to decrease as the angle of attack of the plate surface is varied from -10° (expansion) to $+10^\circ$ (compression). The actual surface static pressure for expansion angles of attack are lower than for compression angles of attack of the test surface.

It may be noted from figures 4 and 6 that the pressure at s/d greater than about 15 are lower than inviscid wedge values. This type of variation may be caused by trailing-edge effects and side boundary effects. Data obtained at two span locations on the unswept model are presented in figure 7 for 0° and 10° angle of attack. A small systematic change is noted in figure 7 for the two span locations. These data seem to indicate that a small side boundary effect is present.

The surface static pressures measured for the present test conditions are compared in figure 8 to the values calculated using equation (11). The empirical constants in equation (11) were taken to be $A = 1/\sqrt{C_w}$ and $B = (1/2)^{2/3}$. In addition, some data obtained by Bogdonoff and Vas (refs. 11 and 12) at M_∞ of 13.3 in helium, by Erickson (ref. 13) at M_∞ of 16 and 17.3 in helium and by Feller (ref. 14) at M_∞ of 6.9 in air are also presented in figure 8. The solid line represents one-to-one correspondence of theory and experiment. It is pointed out that the data are correlated over a range of Mach numbers from 4 to 17.3, leading-edge Reynolds numbers from 600 to 270,000, angles of attack $+10^\circ$ to -10° , angles of sweep from 0° to 60° , and for air and helium. The assumption that the viscous and inviscid flow fields do not interact to a first approximation was made in the analysis. This assumption was also utilized in reference 14 wherein similar correlating factors were obtained. The success of this correlation evidenced by figure 8 indicates that this "independence" assumption is sufficiently good to allow calculation of the surface pressures by the proposed method (eq. (11)) with an average error of ± 8 percent over a wide range of conditions.

Flow Field Surveys

Local flow properties.- A typical impact pressure survey through the flow field above a blunt plate is presented in figure 9. It may be noted that the measured impact pressure increases with distance above the plate, reaches a peak value at the shock wave, and then decreases rapidly to the free-stream impact pressure. Similar survey results have been reported in references 7, 8, 9, 15, and 16. As in reference 7, the boundary-layer edge was defined here as the point where the impact pressure curve has approached within 1 percent of the linear portion as noted in figure 9. The Mach number distributions for this flow field survey were calculated on the assumption that the static-pressure gradient normal to the surface through the boundary layer was negligible. The velocity distribution was calculated on the additional assumption that total temperature was constant. From figure 10, one can observe that the local Mach number and velocity at the boundary-layer edge are lower than the undisturbed free-stream values. This effect of leading-edge blunting will be discussed in a later section.

Shock-wave shape.- The shape of the shock wave generated by the leading edge has been assumed in the analysis section to depend only on conditions at the leading edge. In order to assess this assumption, shock-wave shapes were obtained from surveys of the flow over a blunt plate at a Mach number of 5.7 and leading-edge Reynolds number of 4860 for various angles of sweep and angles of attack. The shock-wave heights are plotted in figure 11 as a function of dimensionless distance from the leading edge. As expected, these data exhibit differences due to angle of sweep. The results of the analysis indicate that the effect of sweep introduces a factor of $\cos \Omega$ in equation (10). However, the present data for various sweep angles are noted in figure 11 to have little dependence on sweep. One possible fit of the data can be made by use of the factor $\cos^{1/3} \Omega$ in equation (10) rather than $\cos \Omega$. These data are presented in correlated form in figure 12 utilizing the $\cos^{1/3} \Omega$ factor. However, there is no apparent theoretical reason for the use of this factor. In figure 13, the above-mentioned factor of $\cos^{1/3} \Omega$ was used to compare the shock-wave-shape data of the present tests with data obtained for blunt inclined plates and blunt swept plates at a Mach number of 13.3 in helium (refs. 11 and 17), for blunt plates at a Mach number of 4 in air (ref. 7), and for sharp plates at a Mach number of 5.7 in air (ref. 16). The dimensionless distances plotted on the abscissa of figure 13 may be noted to include the bow wave detachment distances as obtained from reference 18. These detachment distances have an appreciable effect at small values of s/d . In contrast, this refinement is negligible for s/d values above 20.

The effects of angle of surface inclination are noted to be negligible for shock heights, R , (measured to the 0° inclination center line) for both the present test data and the data for $M_\infty = 13.3$. Also shown in figure 13 are two solid lines representing a parabolic and a linear variation of the shock-wave shape with distance. The data near the leading edge are noted to be fit well by the square root (or parabolic) variation. Far from the leading edge the shock wave approaches a linear variation with distance from the leading edge. The blast wave prediction of a $2/3$ -power variation is shown to fit these data from an $(s/d + \Delta/d)$ of 2 to 50 by the following equation:

$$\frac{R}{d \cos^{1/3} \Omega} = 1.3 \left(\frac{s}{d} + \frac{\Delta}{d} \right)^{2/3} \quad (17)$$

Boundary-layer thickness.- Boundary-layer thicknesses obtained as described above, and noted in figure 9, are presented in figure 14 plotted as a function of distance from the leading edge. Also presented in figure 14 are two solid curves obtained from the equation (12) using inviscid sharp-wedge conditions. The data obtained for 10° compression inclination of the test surface may be noted to fit the theoretical curve quite well. The data obtained for 0° inclination of the surface and 0°

to 60° of leading-edge sweep are noted to evidence some scatter. However, reasonable fit to the predicted curve is noted for s/d greater than about 4. In figure 15 the data are plotted in a correlation form obtained from equation (12), as:

$$\frac{\delta}{d} \frac{\sqrt{\text{Re}_\alpha d}}{B_1} = \sqrt{\frac{s}{d}} \quad (18)$$

where

$$B_1 = \left[\frac{1.73}{M_\alpha^2} \frac{T_w}{T_\alpha} + 0.332(\gamma-1) + \frac{4.27}{M_\alpha^2} \right] M_\alpha^2 \sqrt{C_w}$$

Also presented in figure 15 are data obtained by Kendall (ref. 16) for a very sharp leading-edge plate at a Mach number of 5.8 for zero angle of sweep and the data obtained for sharp plates from the present tests. The solid line plotted in figure 15 is the square-root variation with distance from the leading edge prescribed by equation (18). The data are noted to be correlated quite well by this infinitely sharp leading-edge equation over a range of leading-edge Reynolds numbers from 12 to 6600. Note here also that variation of the sweep of the blunt leading edge from 0° to 60° has no appreciable effect on the boundary-layer thickness. This correlation indicates that the boundary-layer thickness is independent of leading-edge bluntness and leading-edge sweep. This result substantiates the assumption made in the Analysis section that the viscous contribution to the surface pressure may be calculated independently of bluntness or sweep.

In general, the flow field surveys discussed here indicate that for blunt plates in hypersonic flow the leading-edge dominates the inviscid flow field and that the boundary-layer growth proceeds unaffected by either the leading-edge bluntness or sweep. These results tend to substantiate the assumption that the viscous and inviscid flows do not interact insofar as the parameters necessary to surface static-pressure calculation are concerned.

Local Reynolds Number

The Reynolds number parameter calculated for local conditions depends on values of the local flow properties such as total pressure, Mach number, and temperature along the boundary-layer edge, as may be noted in equation (16). The boundary-layer edge or flow-field surveys described above were utilized to obtain these local properties. The effect of the variation of these local properties on the local Reynolds number will be described.

The local total pressures along the boundary-layer edge may be calculated from the measured local impact pressures and local surface static pressures. The assumptions involved are that the static-pressure gradient through the boundary layer is negligible and a detached bow shock exists in front of the impact pressure probe. The results of this calculation for the present tests are presented in figure 16, wherein the ratio of calculated local total pressure to free-stream total pressure is plotted as a function of sweep angle. Data are also presented for conditions where the surface inclination is different from zero. The solid line in figure 16 is the variation predicted by means of oblique shock-wave theory (eq. (13)). The agreement of the data with the solid line indicates that variation of local total pressure with sweep may be predicted with fair accuracy. The variation in the measured total pressure with distance from the leading edge was small as may be noted from figure 16. Therefore, these tests are not indicative of the maximum downstream extent of the effect of the high entropy layer of gas caused by the detached bow shock wave.

The local Mach number at the boundary-layer edge was calculated by means of the measured surface pressure and measured impact pressure. The results for typical test conditions are shown in figure 17, wherein the ratio of local to free-stream Mach number is plotted versus distance from the leading edge. The local Mach numbers are lower than the free-stream value. The increase of the local Mach number with distance from the leading edge is due to the decrease in static pressure with distance. The values are also noted in figure 17 to increase, and approach the free-stream value of Mach number, as sweep of the leading edge is increased. This increase in local Mach number with sweep reflects the variation in the surface static pressure and total pressure at the boundary-layer edge caused by sweep of the leading edge.

As previously stated, when certain local flow quantities are known, the local Reynolds number can be calculated by means of equation (14). This calculation was made for the present test conditions for which these properties were measured. The effect of variation of free-stream Mach number and sweep on local Reynolds numbers are shown separately in figures 18 and 19, respectively. In figure 18, the ratio of local to free-stream Reynolds number is plotted versus dimensionless distance from the leading edge for zero sweep of the plate leading edge. The data shown were obtained at Mach number of 5.7 for the present tests and at a Mach number of 3.95 from reference 7. This ratio of Reynolds numbers does not depend on the Reynolds number of the leading edge for that range of conditions where the reduction of the total pressure is known, as was pointed out in reference 7. It can be seen from figure 18 that the variation in local Reynolds number with free-stream Mach number is predicted by equation (15) wherein $\omega = 1$ and $\zeta = 0.57$ for the temperature range of the tests. The predominant factor causing the difference in level of these curves is the total-pressure ratio across the detached bow shock wave.

The effect of leading-edge sweep on local Reynolds numbers is shown parametrically in figure 19, wherein the Reynolds number ratio is plotted versus s/d . The local Reynolds number is noted to approach free-stream value (inviscid sharp flat plate value) as the sweep of the leading edge is increased. Again, for these test conditions, it is noted from equation (15) and figure 19, that the dominating factor in this variation of level is the local total pressure. The upper dashed line plotted in figure 19 was calculated for zero leading-edge sweep using the known surface pressures and a local total pressure assumed equal to the free-stream value. The solid curves were calculated from equation (15) with local total pressures obtained from equation (13) and with measured values of surface pressure. Comparison of the dashed curve with the data for the case of zero leading-edge sweep (circular symbols) points out that the assumption of no reduction in total pressure might well lead to quite erroneous results for the local Reynolds number. In fact, an error of nearly 800 percent could be encountered for these conditions. The surface pressures and the local total pressures must both be known before an accurate calculation of local Reynolds number can be made.

CONCLUSIONS

Experimental studies were made of the effect of leading-edge sweep and angle of attack on the hypersonic flow field over blunt flat plates. In particular, pressures were measured over blunt flat plates at nominal Mach numbers of 4.0 and 5.7 at free-stream Reynolds numbers of 6,600 and 20,000 per inch.

These surface pressures were predicted to engineering accuracy by a method developed herein utilizing a combination of viscous and inviscid hypersonic parameters. Furthermore, this method was found to predict surface pressure results obtained in other similar investigations. In fact, the applicability to wind-tunnel tests was found to encompass a range of Mach numbers from 4 to 17.3, free-stream Reynolds numbers per inch from 6,600 to 1,000,000, leading-edge thicknesses from 0.0006 to 0.5 inch, leading-edge sweep from 0° to 60° , surface inclination from 10° expansion to 10° compression, and for both helium and air as the test gases.

The boundary-layer thickness was found to be essentially unaltered by the sweep or bluntness of the leading edge. Results of compressible boundary-layer theory for ideally sharp flat plates were used to predict the boundary-layer growth over blunt plates for Mach numbers from 4 to 5.7 and free-stream Reynolds numbers per inch of 6,600 to 20,000.

The shock-wave shape was changed little by the sweep of the leading edge and by angle of attack. The theoretical variation predicted by an extension of the blast-wave analogy was not in agreement with experiment.

For conditions of leading-edge sweep, total pressures measured along the boundary-layer edge were in agreement with total pressures calculated behind a normal shock wave occurring at the component or crossflow Mach number. For the conditions of the tests described, including angle of attack, the boundary layer had not emerged from the high entropy layer produced by the blunt leading edge.

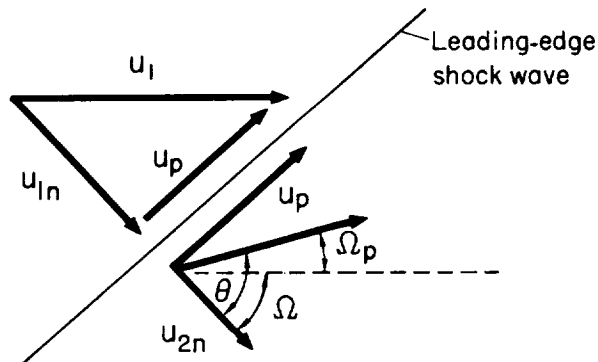
The local Reynolds numbers were reduced by blunting of the leading edge. This reduction was mitigated by sweeping the leading edge.

Ames Research Center
National Aeronautics and Space Administration
Moffett Field, Calif., Sept. 25, 1958

APPENDIX A

LOCAL STREAM ANGLE

A crude estimate of the local stream direction at the edge of the boundary layer on a plate aft of a swept blunt leading edge can be made on the basis of the results of reference 7. The free-stream velocity is separated into components parallel and normal to the leading-edge bow shock wave (sketch (d)) where Ω_p is the angular change of the stream direction.



Sketch (d)

The results of reference 7 indicate that the normal component of velocity when considered alone is reduced by the strong shock wave, and upon re-expansion of the flow to free-stream pressure will reach a value such that $0.8 \leq \frac{u_{2n}}{u_{1n}} \leq 1$.

The lower bound gives rise to the largest stream deflection, thus a value of 0.8 is assumed so that

$$u_{2n} \approx 0.8 u_{1n} \quad (\text{A1})$$

By trigonometry and sketch (d)

$$\tan \theta = \frac{u_p}{u_{2n}} ; \quad \tan \Omega = \frac{u_p}{u_{1n}} \quad (\text{A2})$$

thus,

$$\tan \theta = \frac{\tan \Omega}{0.8} \quad (\text{A3})$$

and

$$\Omega_p = \theta - \Omega \quad (\text{A4})$$

The value of Ω_p will be indicative of the direction of u_2 , the stream velocity, in comparison to free-stream velocity direction. A few values calculated using equations (A3) and (A4) are given below.

<u>Ω,</u> <u>deg</u>	<u>Ω_p,</u> <u>deg</u>
0	0
15	3.5
30	5.8
45	6.4
60	5
90	0

The calculated values of deflection of the stream outside the boundary layer are noted to be small.

REFERENCES

1. Lees, Lester, and Probstein, Ronald F.: Hypersonic Viscous Flow Over a Flat Plate. Aero. Eng. Lab. Rep. 195, Princeton Univ., Apr. 20, 1952.
2. Lees, Lester: On the Boundary Layer Equations in Hypersonic Flow and Their Approximate Solutions. Aero. Eng. Lab. Rep. 212, Princeton Univ., Sept. 20, 1952.
3. Lees, Lester, and Kubota, Toshi: Inviscid Hypersonic Flow Over Blunt-Nosed Slender Bodies. Jour. Aero. Sci., vol. 24, no. 3, Mar. 1957, pp. 195-202. (Also available as GALCIT Memo. 31, Feb. 1, 1956.)
4. Cheng, H. K., and Pallone, A. J.: Inviscid Leading-Edge Effect in Hypersonic Flow. Jour. Aero. Sci., vol. 23, no. 7, July 1956, pp. 700-702.
5. Taylor, G. I.: The Formation of a Blast Wave by a Very Intense Explosion. Proc. Roy. Soc. of London, ser. A, vol. 201, no. 1065, Mar. 1950, pp. 159-186.
6. Sakurai, Akira: On the Propagation and Structure of the Blast Wave, I. Jour. Phys. Soc. Japan, vol. 8, no. 5, Sept.-Oct. 1953.
7. Creager, Marcus O.: Effects of Leading-Edge Blunting on the Local Heat Transfer and Pressure Distributions Over Flat Plates in Supersonic Flow. NACA TN 4142, 1957.
8. Brinich, Paul F.: Effect of Leading-Edge Geometry on Boundary-Layer Transition at Mach 3.1. NACA TN 3659, 1956.
9. Crawford, Davis H., and McCauley, William D.: Investigation of the Laminar Aerodynamic Heat-Transfer Characteristics of a Hemisphere-Cylinder in the Langley 11-Inch Hypersonic Tunnel at a Mach Number of 6.8. NACA TN 3706, 1956.
10. Penland, Jim A.: Aerodynamic Characteristics of a Circular Cylinder at Mach Number 6.86 and Angles of Attack up to 90° . NACA TN 3861, 1957.
11. Bogdonoff, S. M., and Vas, I. E.: Preliminary Study of the Flow Over a Blunt Flat Plate at Various Angles of Attack at $M=13.3$. Part II: Study of an Elliptical Leading Edge. Bell Aircraft Corp. Rep. D143-978-005, Oct. 1, 1956. (Also available as ARDC-TR-56-41 and ASTIA AD-1131-079.)

12. Bogdonoff, S. M., and Vas, I.E.: The Effect of Sweep Back Angle on the Pressure Distribution of a Blunt Flat Plate at Hypersonic Speeds. Part I: Studies of a Hemicylindrical Leading Edge Flat Plate at Angles of Attack, $\Omega=45^\circ$ and $M_1 \sim 13.3$. Bell Aircraft Corp. Rep. D143-978-011, June 7, 1957.
13. Erickson, Wayne D.: Study of Pressure Distributions on Some Simple Sharp-Nosed Models at Mach Numbers of 16 to 18 in Helium Flow. NACA TN 4113, 1957.
14. Bertram, Mitchel H., and Henderson, Arthur, Jr.: Effects of Boundary-Layer Displacement and Leading-Edge Bluntness on Pressure Distribution, Skin Friction, and Heat Transfer of Bodies at Hypersonic Speeds. NACA TN 4301, 1958.
15. Kubota, Toshi: Investigation of Flow Around Simple Bodies in Hypersonic Flow. GALCIT Memo. 40, June 25, 1957.
16. Kendall, James M., Jr.: Experimental Investigation of Leading-Edge Shock Wave-Boundary Layer Interaction at Hypersonic Speeds. IAS Preprint 611, 1956. (Also available as GALCIT Memo. 30, Jan. 1956.)
17. Bogdonoff, Seymour M., and Vas, I. E.: A Preliminary Study of the Effect of Sweptback Angle on Shock Shape at Hypersonic Speeds. Bell Aircraft Corp. Rep. D143-978-003, June 29, 1956. (Also available as ARDC TR 56-70.)
18. Liepmann, H. W., and Roshko, A.: Elements of Gas Dynamics. GALCIT Aeronautical Series, John Wiley and Sons, Inc., New York, 1957.

TABLE I.- STREAM CONDITIONS

Design Mach No.	Test Mach No.	Static pressure Microns of Hg	Re_{∞} /inch	Usable diameter of stream, in.
4	3.95	300	6,600	3.6
6	5.7	250	20,000	2

TABLE II.- SUMMARY OF TEST CONDITIONS

Type of test	M_{∞}	$Re_{\infty d}$	\bar{d} , in.	α	Ω
Surface pressure and flow-field surveys	5.7	4860	0.25	0	0
	↓	↓	↓	↓	30
				↓	45
				↓	60
				10	0
Surface pressures	5.7	4860	.25	2	0
	↓	↓	↓	4	↓
				6	
				8	
				10	30
			-10	30	
Surface pressure and flow-field surveys	5.7	40	.002	0	0
	↓	↓	↓	↓	60
Surface pressures	3.95	3300	.5	-10	0
	↓	↓	↓	-6	↓
				0	
				6	
				10	

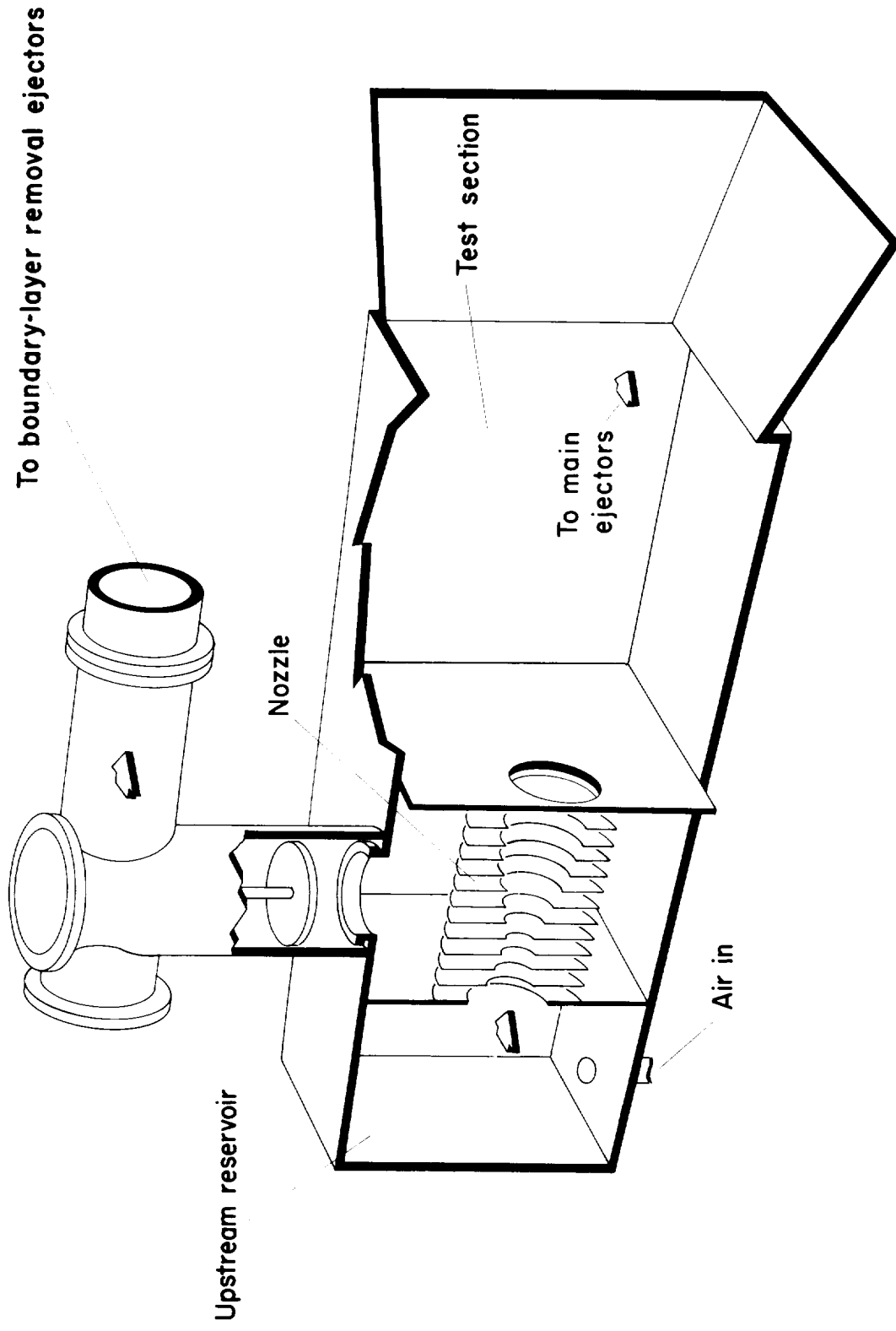
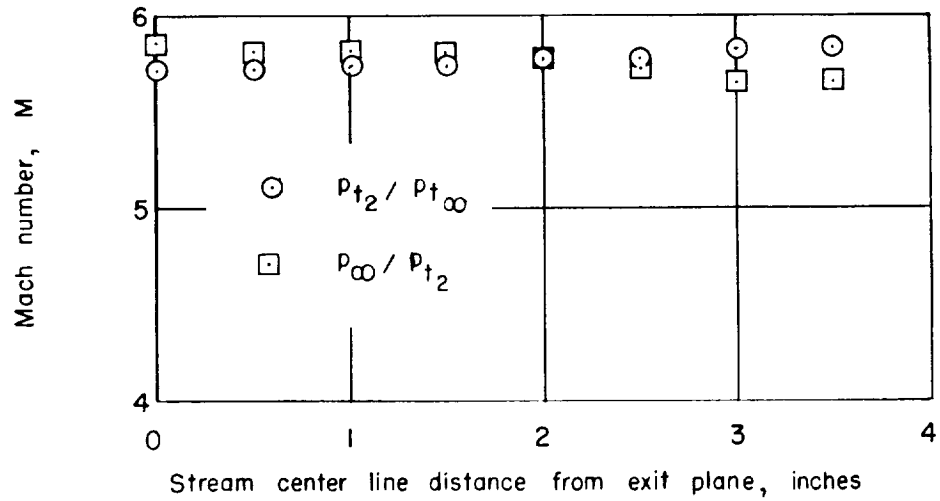
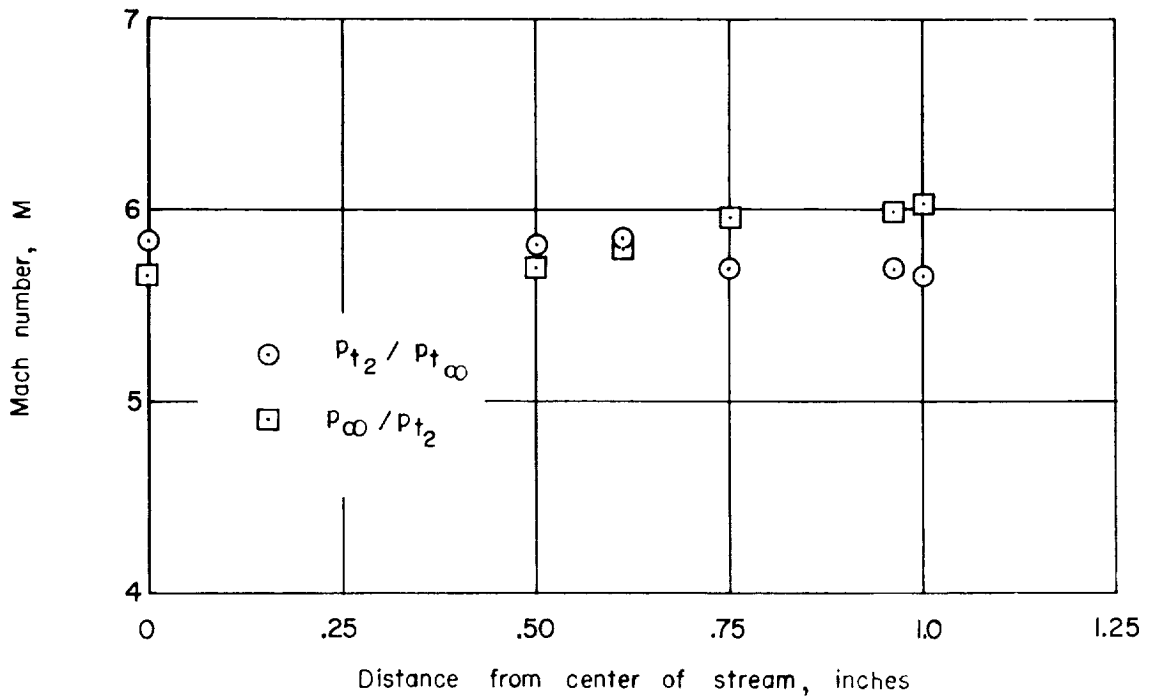


Figure 1.- General arrangement of wind tunnel.

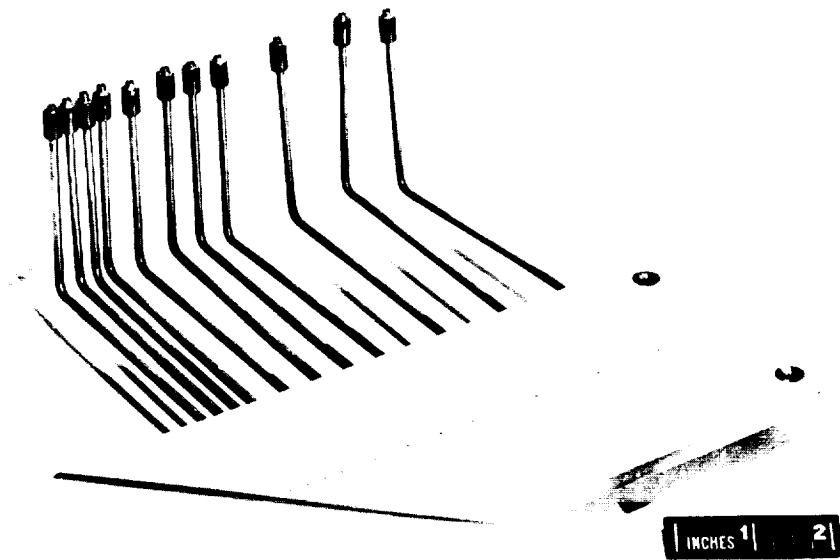


(a) Survey along center line.



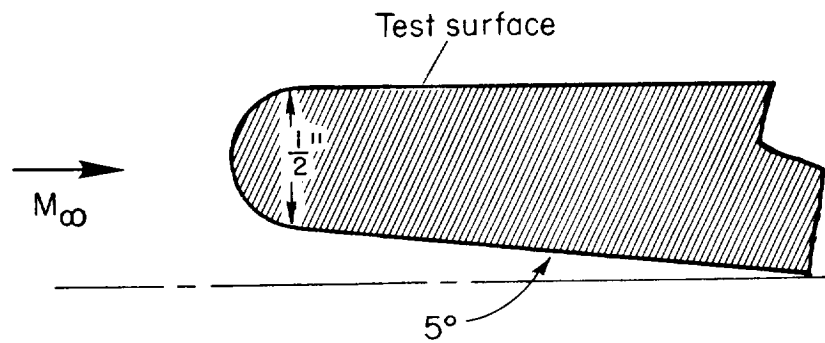
(b) Survey at a station 3.5 inches downstream of nozzle exit plane.

Figure 2.- Comparison of free-stream Mach number calculated by two methods from surveys of the Mach number 6 jet.

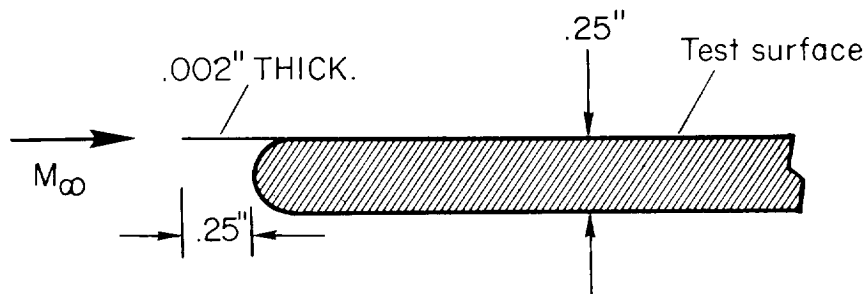


(a) Test body with 45° swept leading edge.

A-23681



(b) Section of unswept body tested in the Mach number 4 stream.



(c) Section of thin leading-edge body.

Figure 3.- Test bodies.

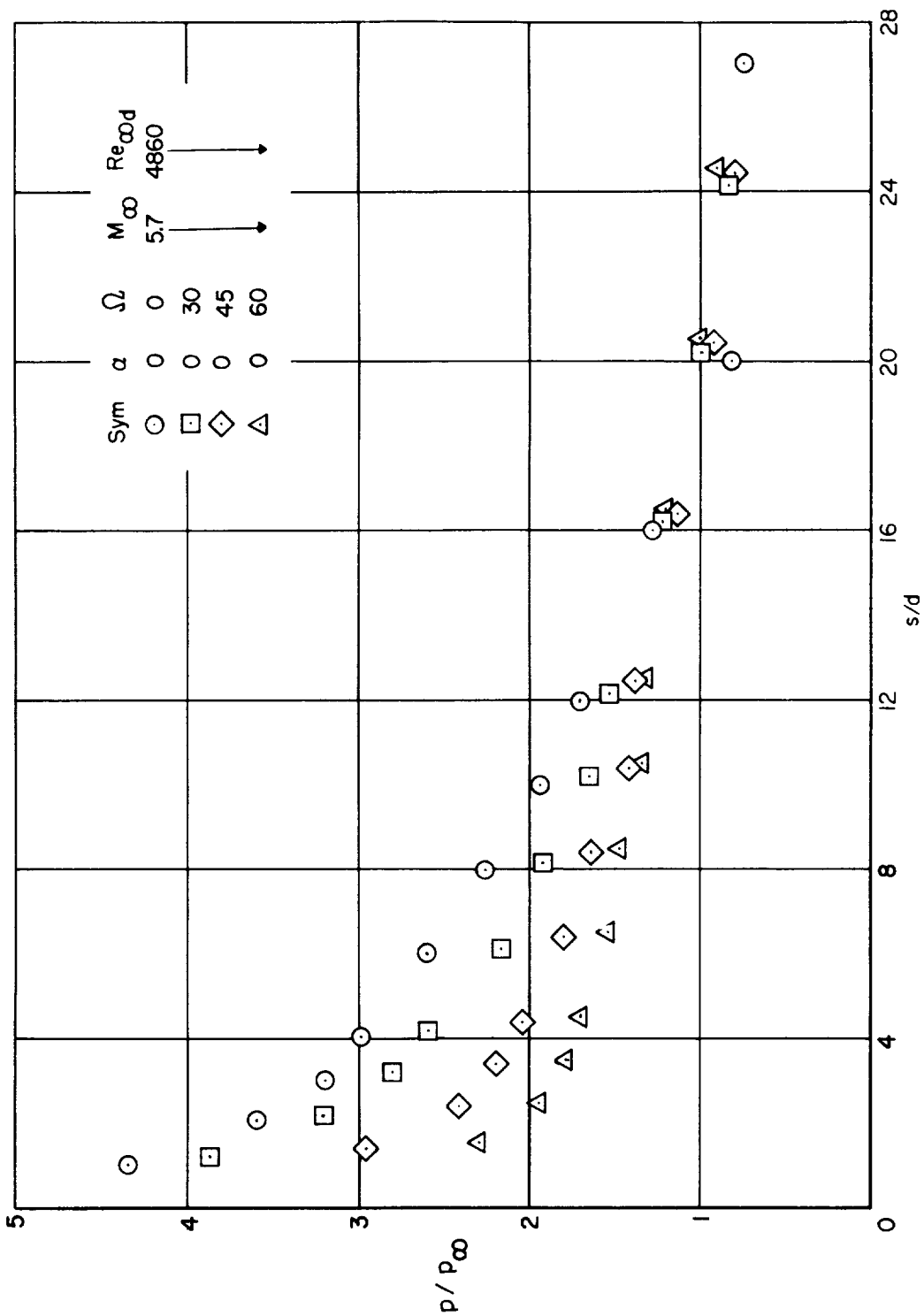


Figure 4.- Variation of the ratio of surface pressure to free-stream pressure with streamwise distance from the swept leading edge of blunt plates.

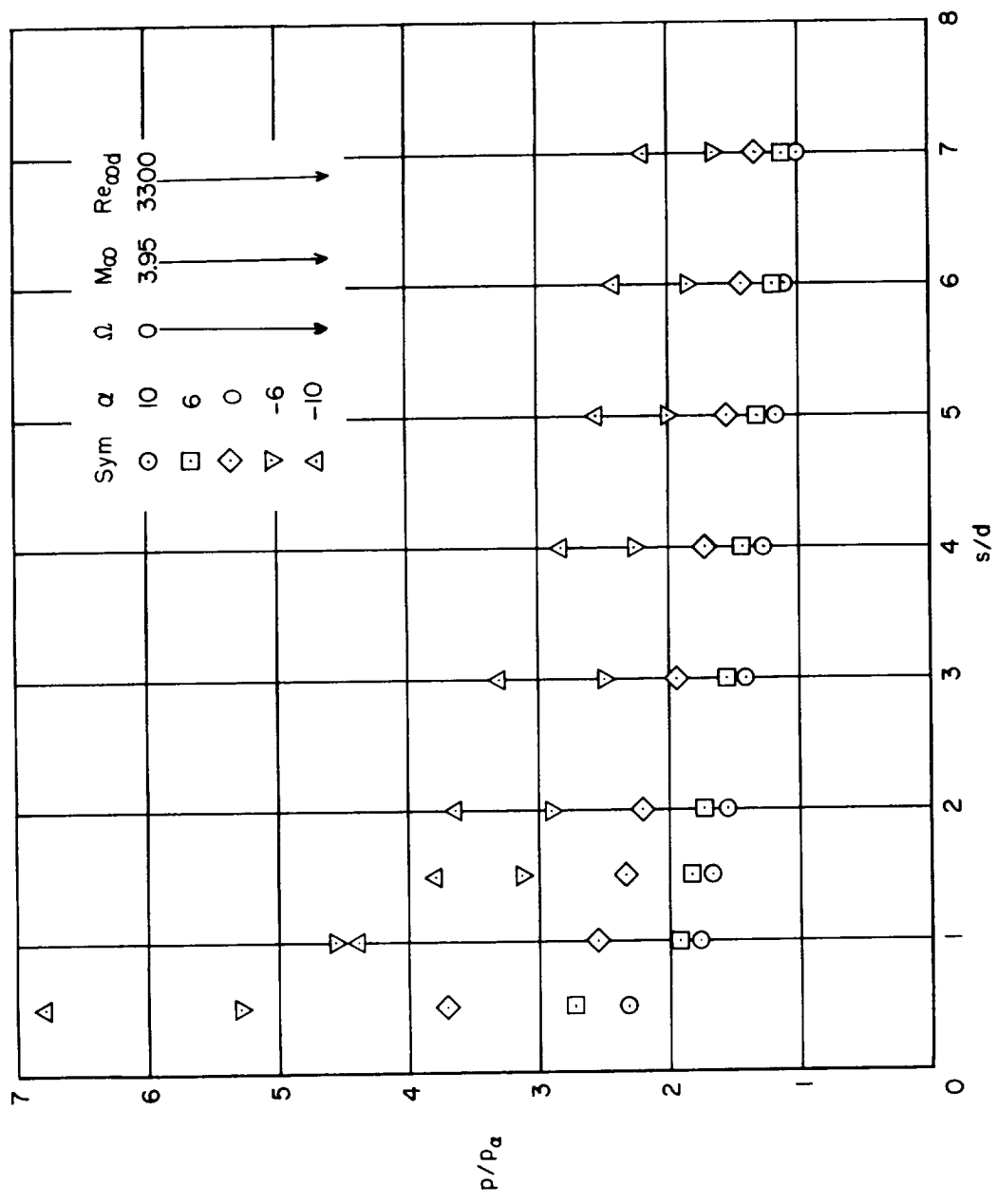


Figure 5.- Variation of the ratio of surface pressure to inviscid sharp wedge pressure with distance from the leading edge of an inclined flat plate.

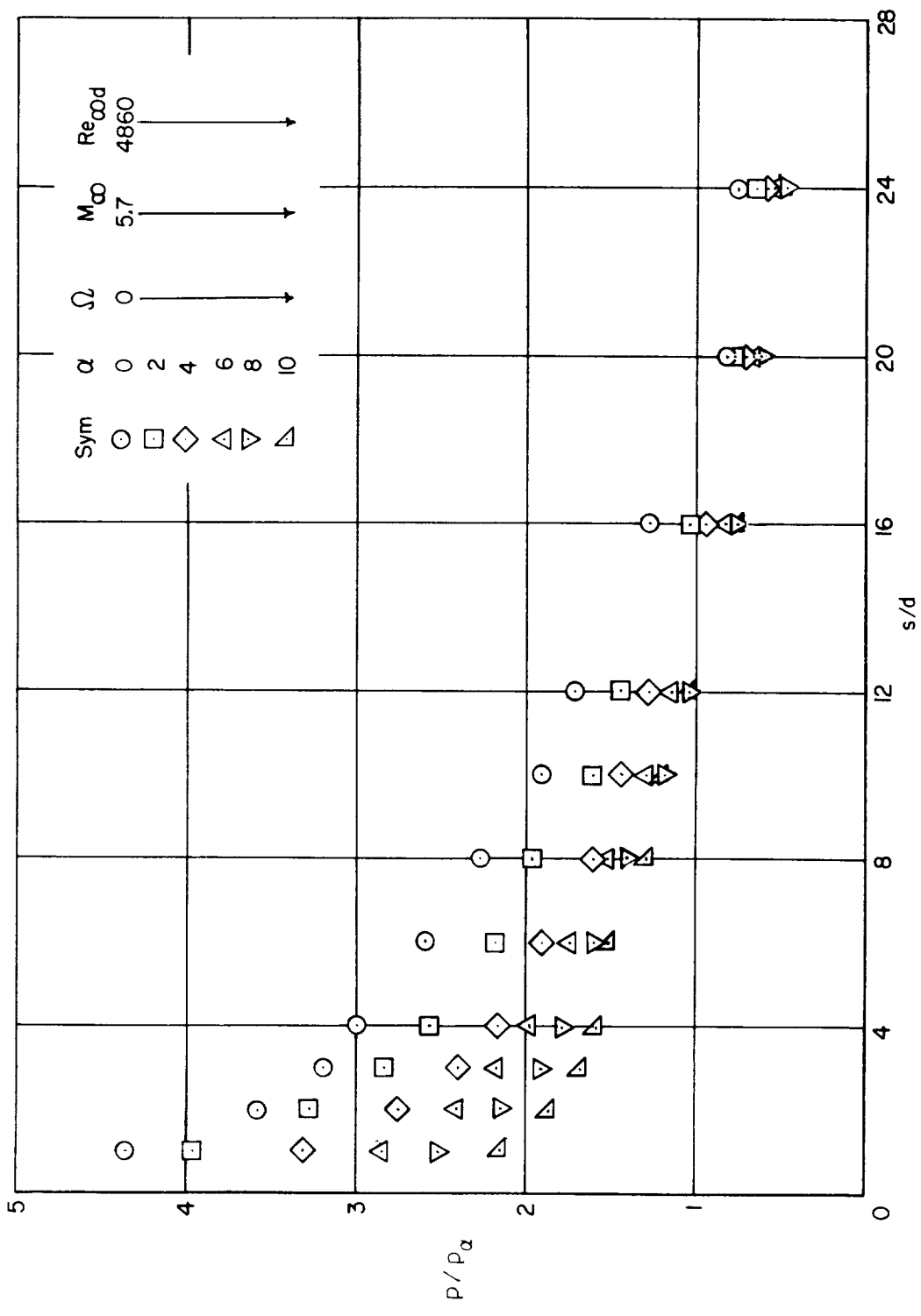


Figure 6.- Variation of the ratio of surface pressure to inviscid sharp wedge pressure with distance from the leading edge of an inclined plate.

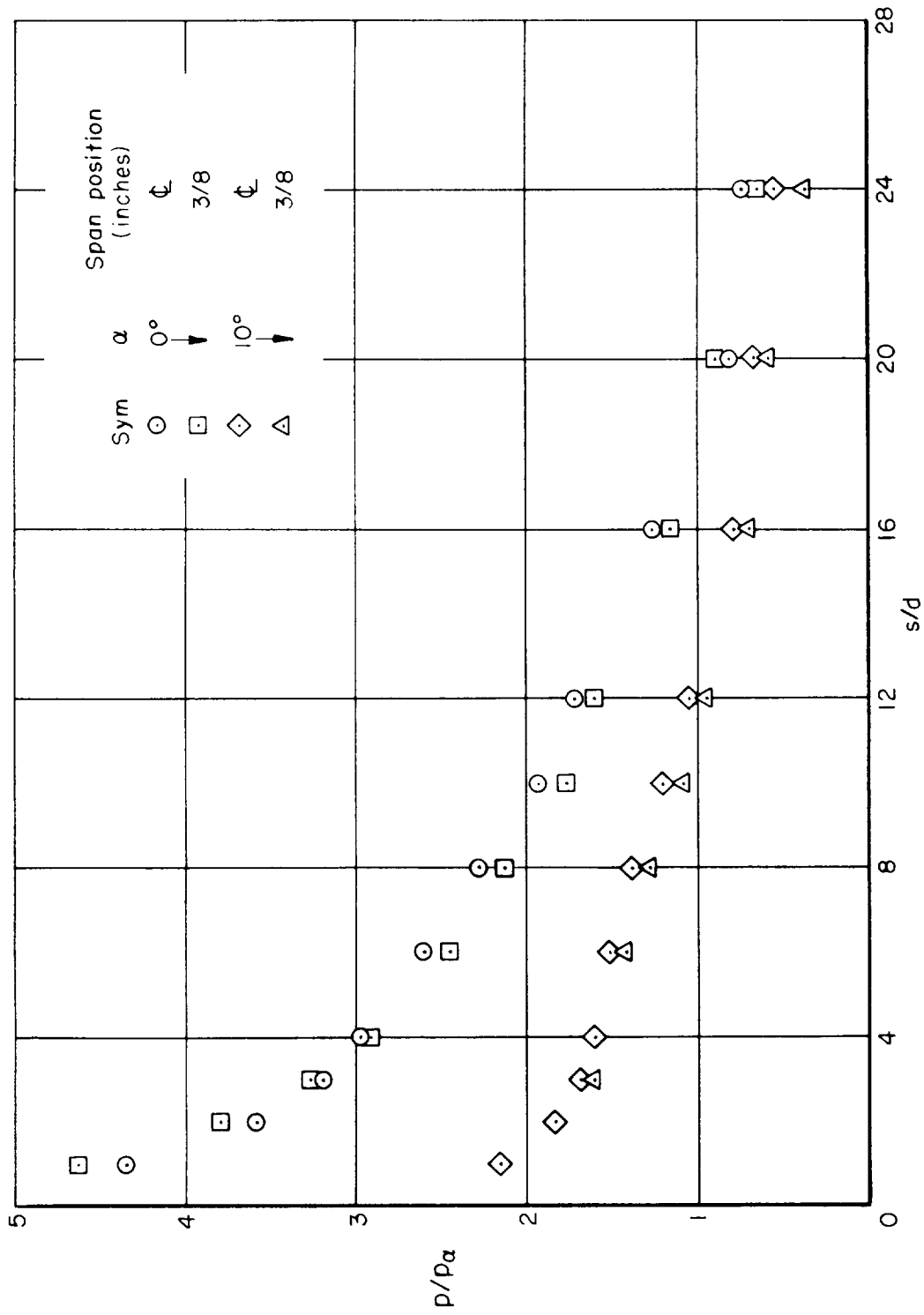


Figure 7.- Variation in surface pressure distribution with span location on an unswept blunt plate; $M_\infty = 5.7$, $Re_{rod} = 4860$.

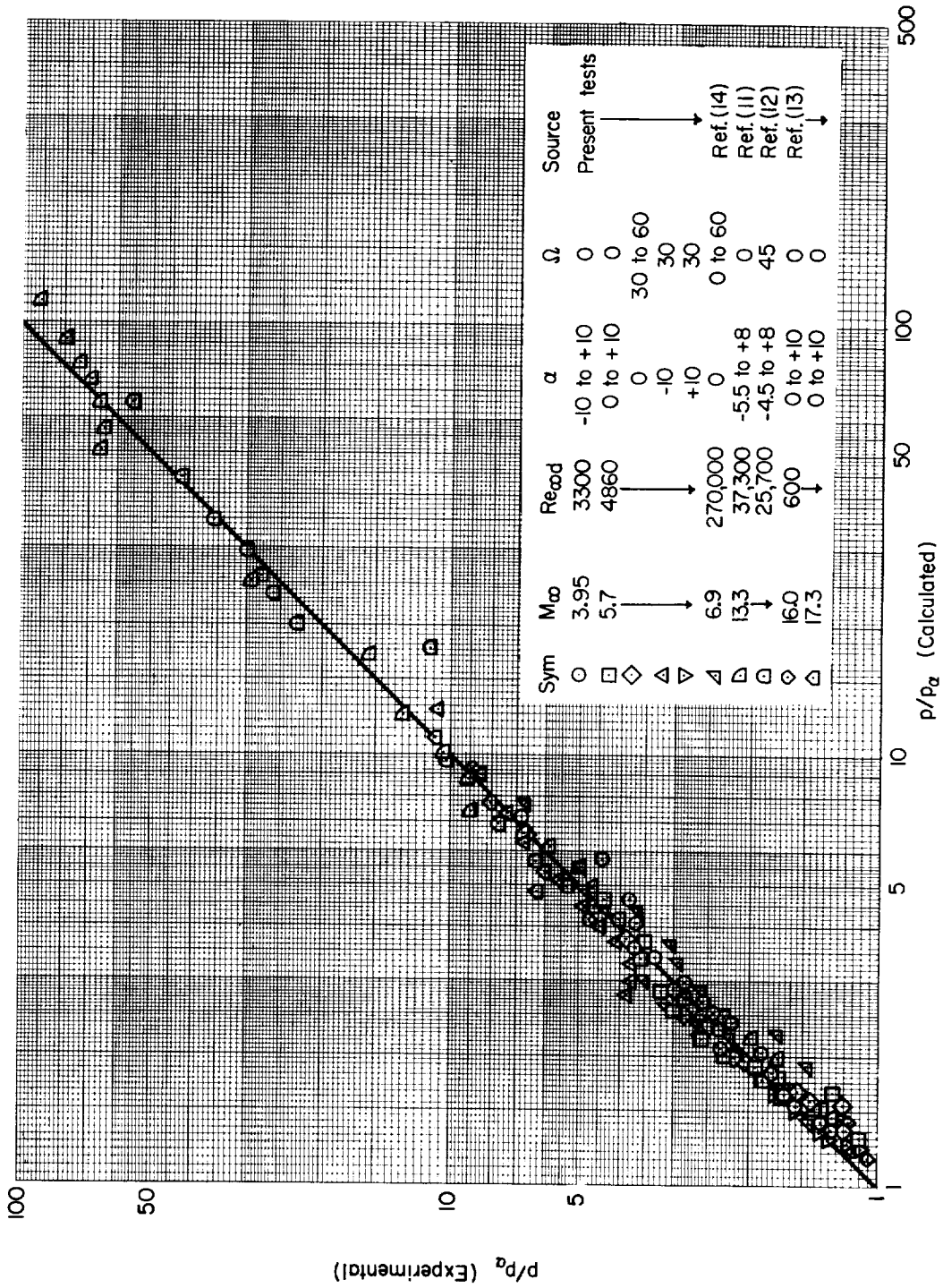


Figure 8.- Comparison of measured pressure ratio with calculated pressure ratio.

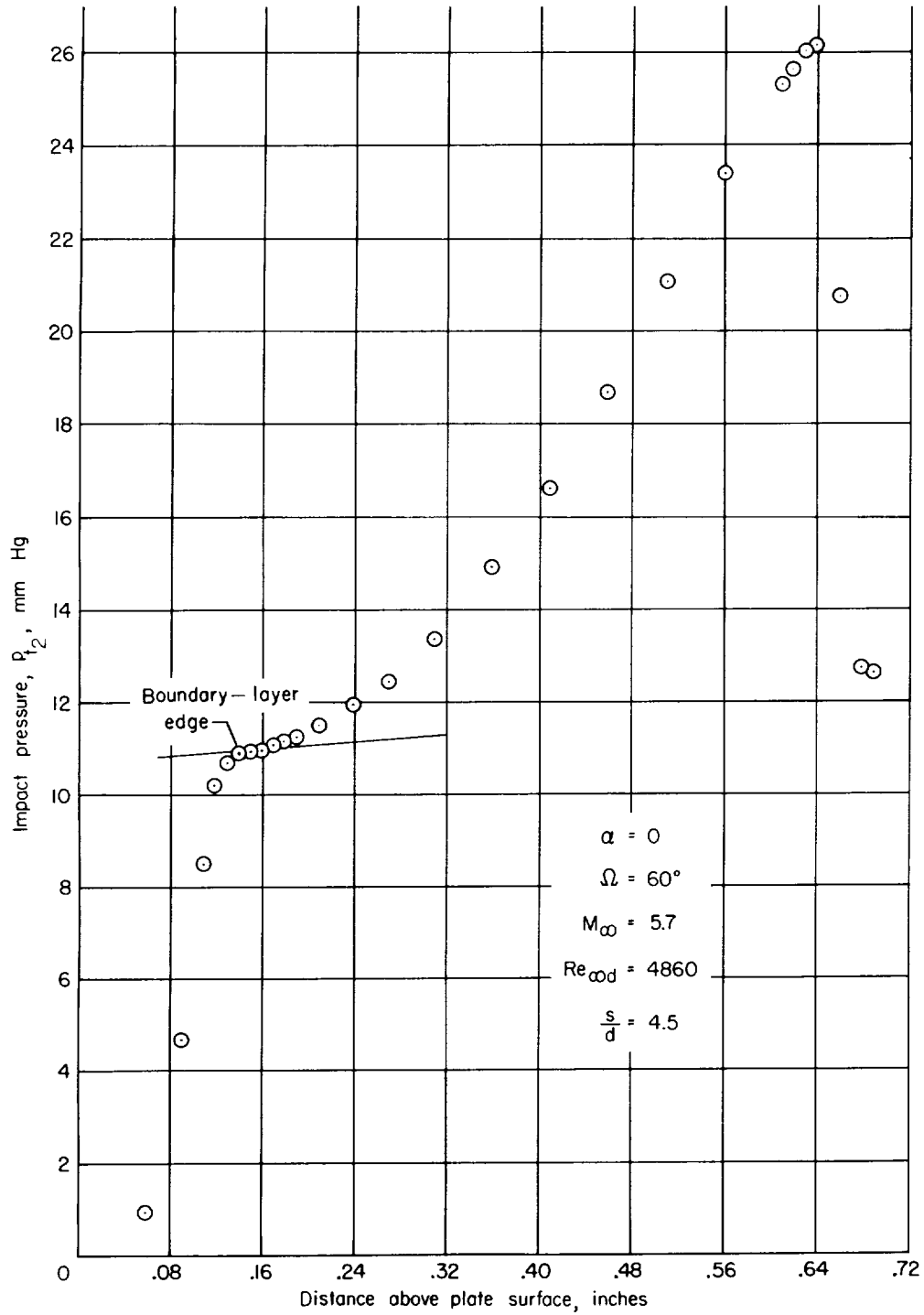


Figure 9.- Variation of impact pressure with height above a blunted plate.

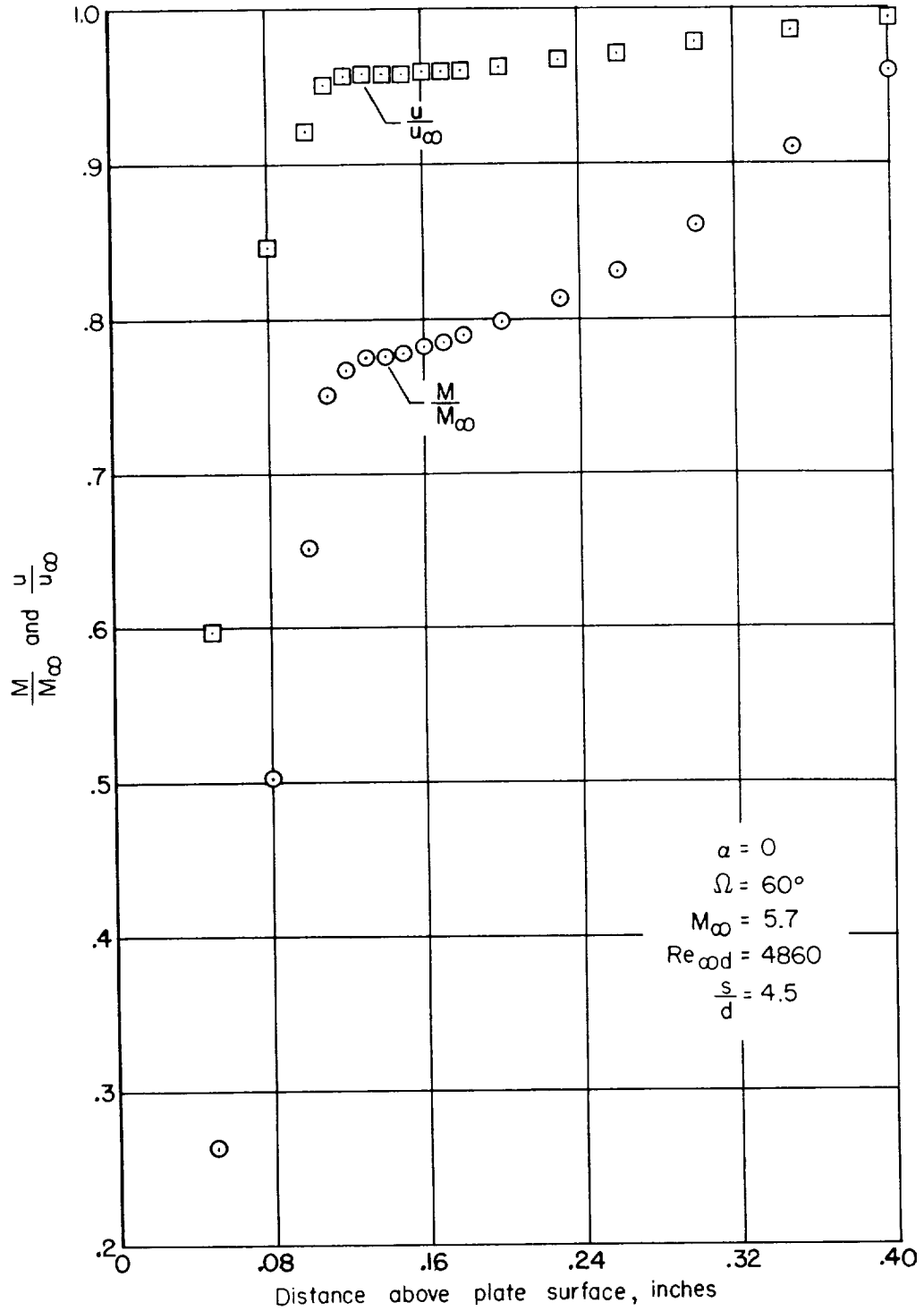


Figure 10.- Variation of Mach number and velocity ratios with height above a blunt plate.

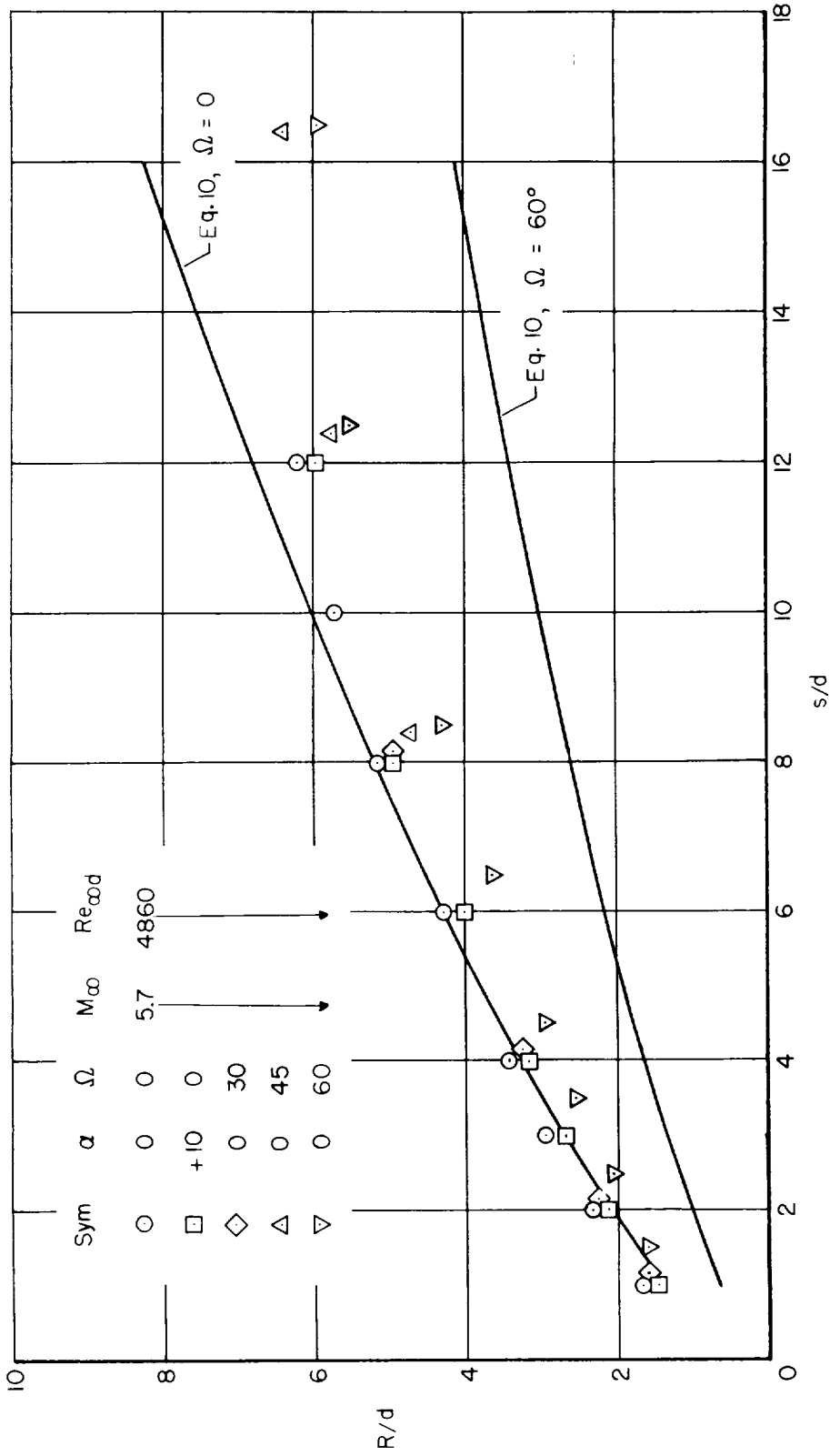


Figure 11.- Variation of measured shock-wave heights with streamwise distance.

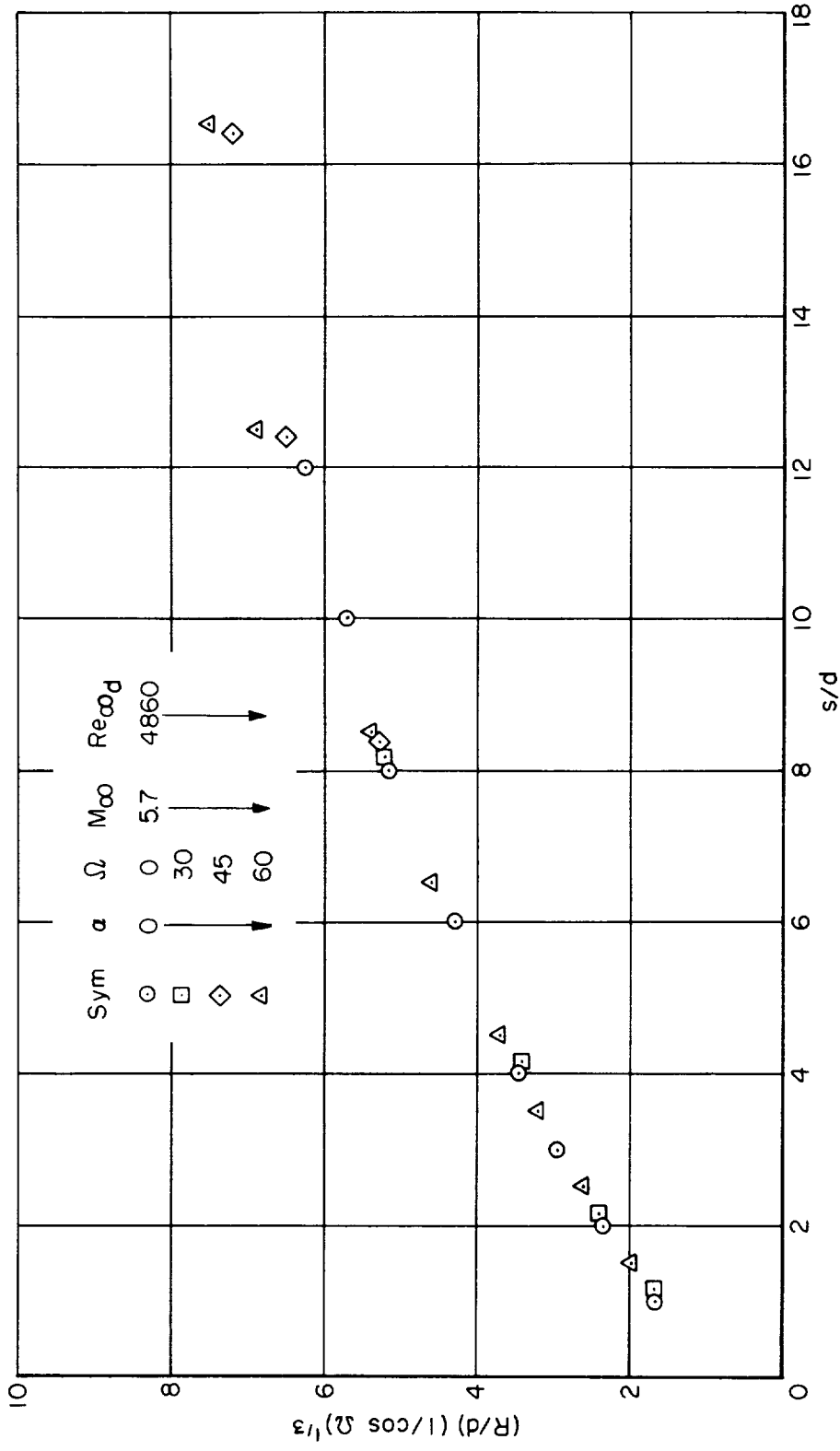


Figure 12.- Correlation of shock-wave position with streamwise distance from the leading-edge of swept blunt plates.

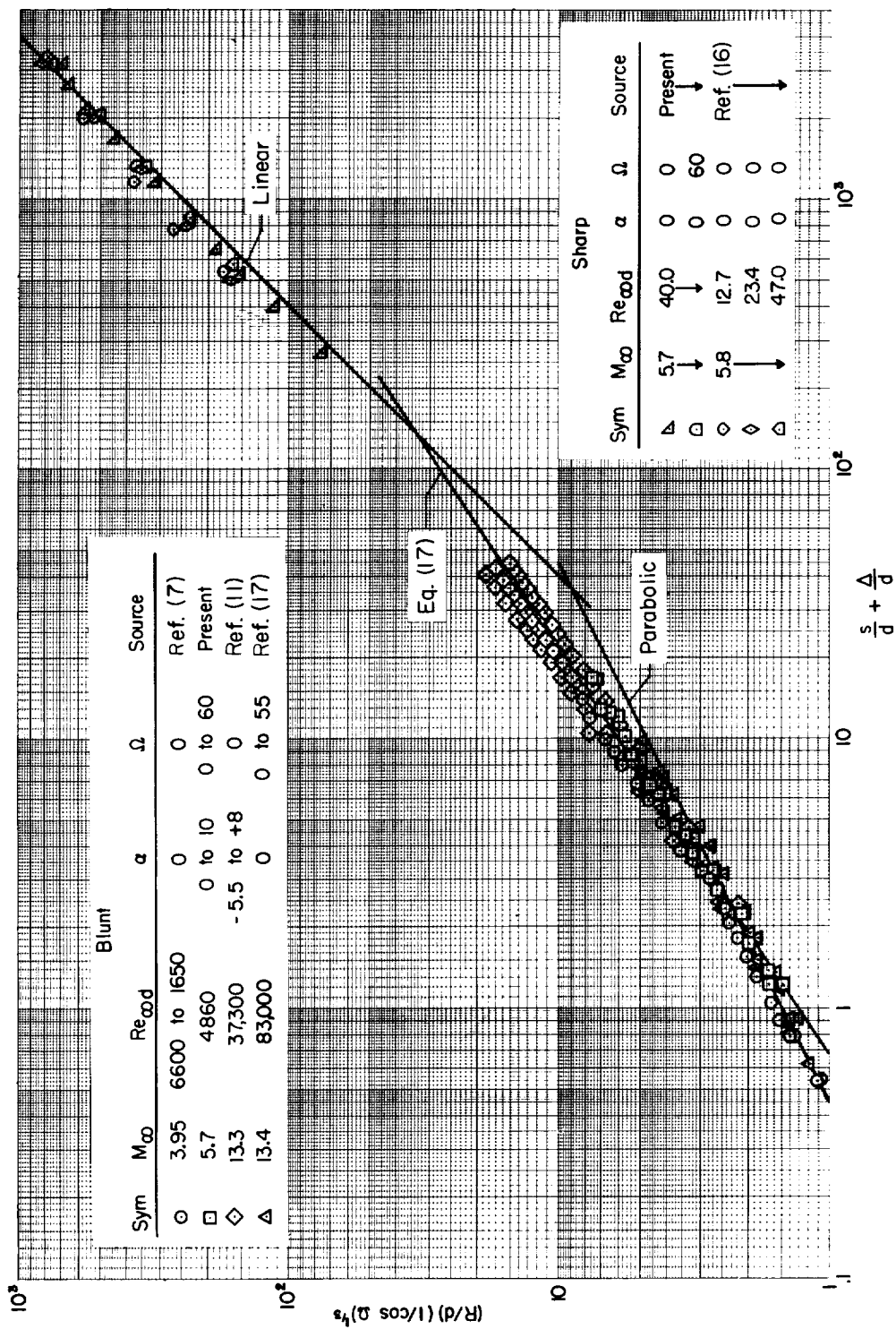


Figure 13.- Correlation of shock-wave heights for blunt and sharp plates.

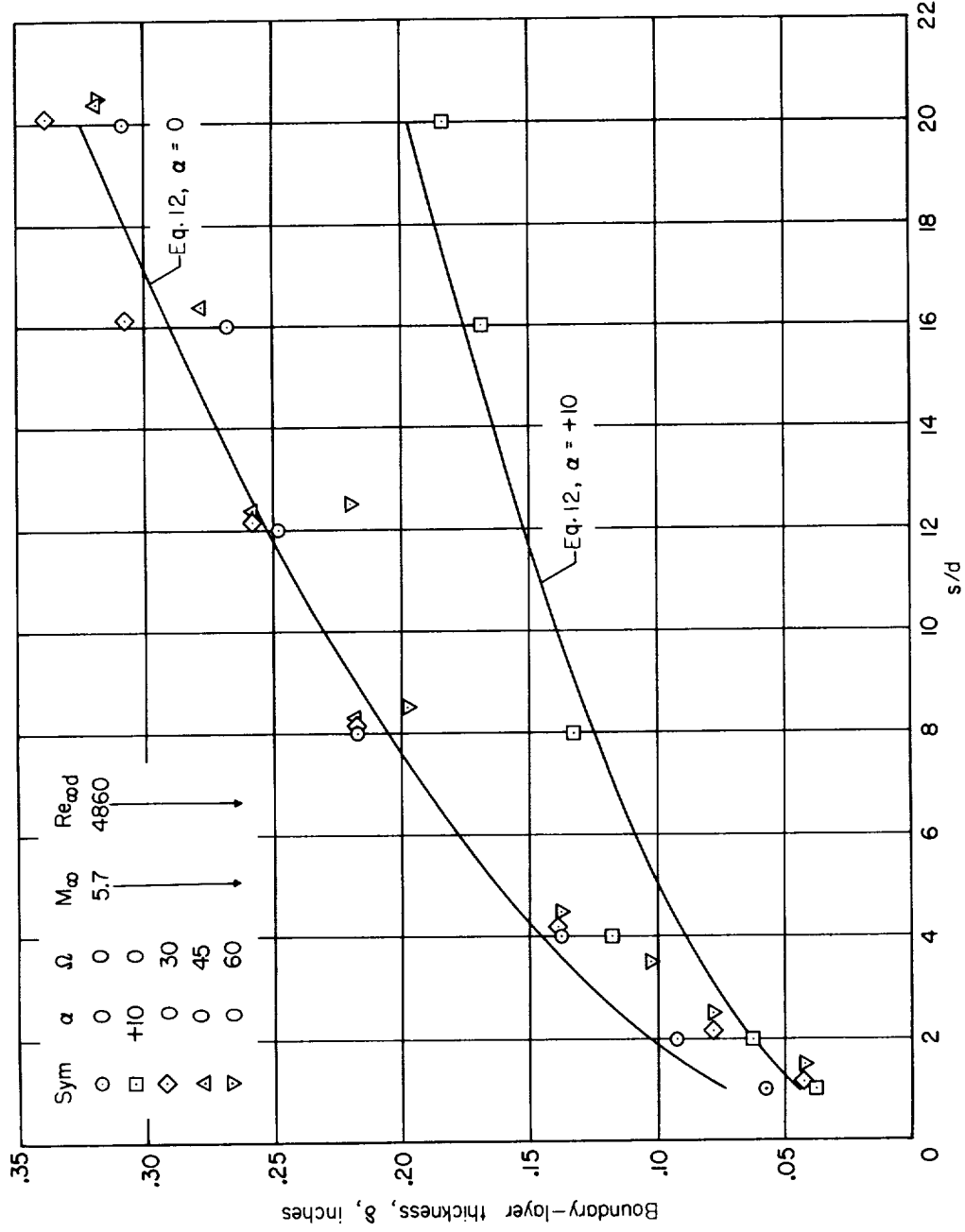


Figure 14.- Variation of the boundary-layer thickness over blunt plates with streamwise distance from the leading edge.

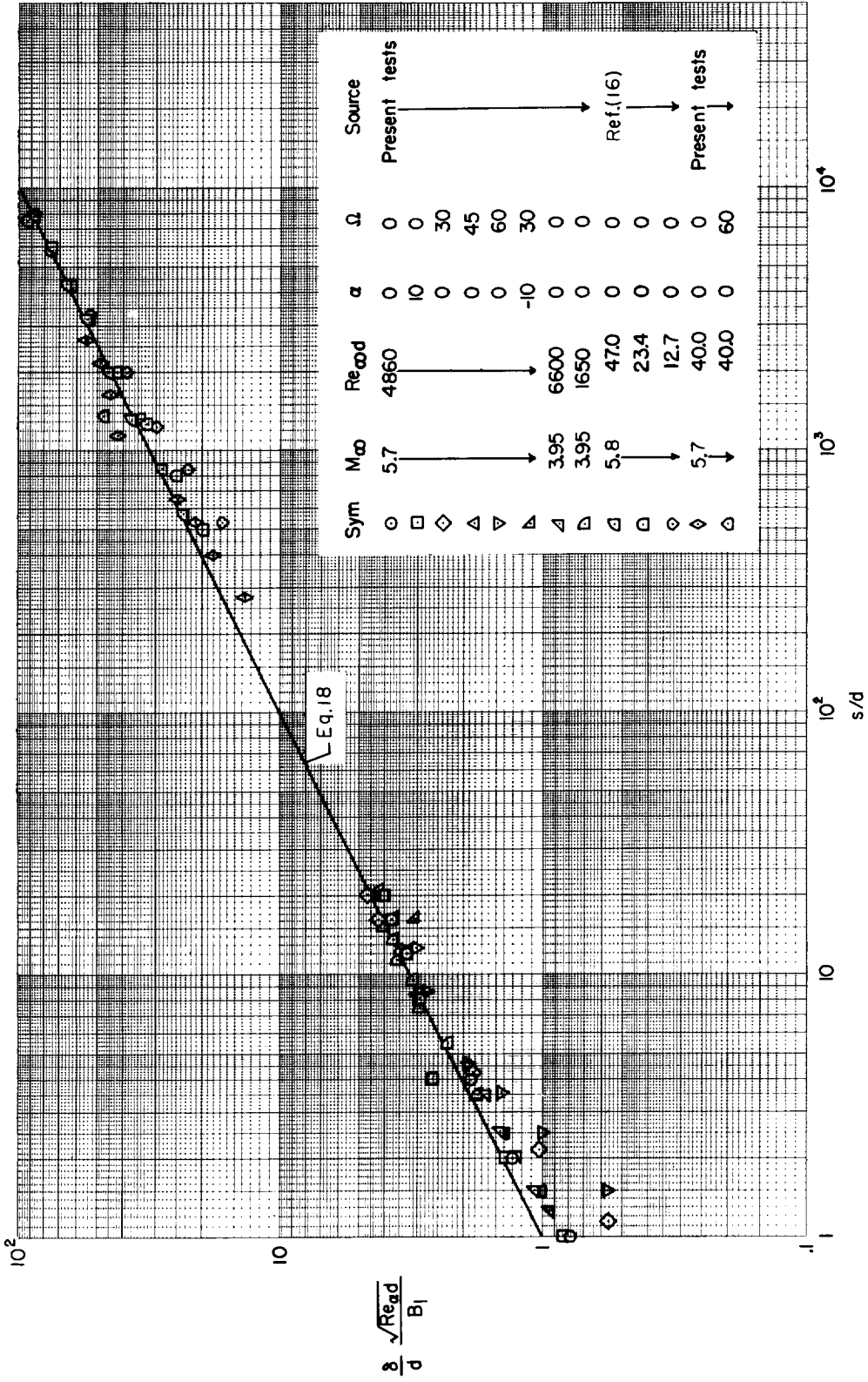


Figure 15.- Correlation of measured boundary-layer thicknesses for blunt and sharp plates.

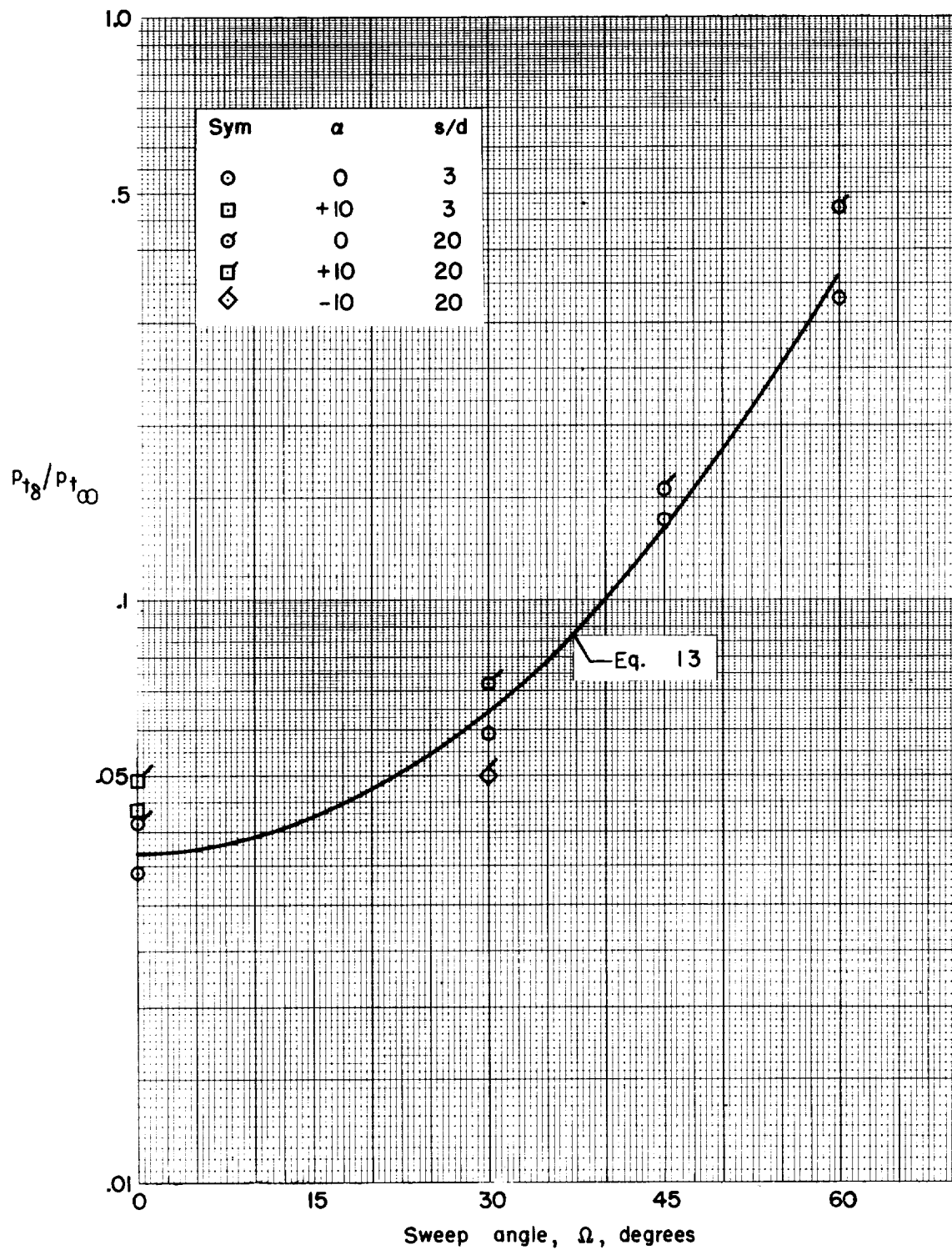


Figure 16.- Variation of the ratio of local total pressure to free-stream total pressure with sweep of the leading edge for $M_{\infty} = 5.7$ and $Re_{\infty d} = 4860$.

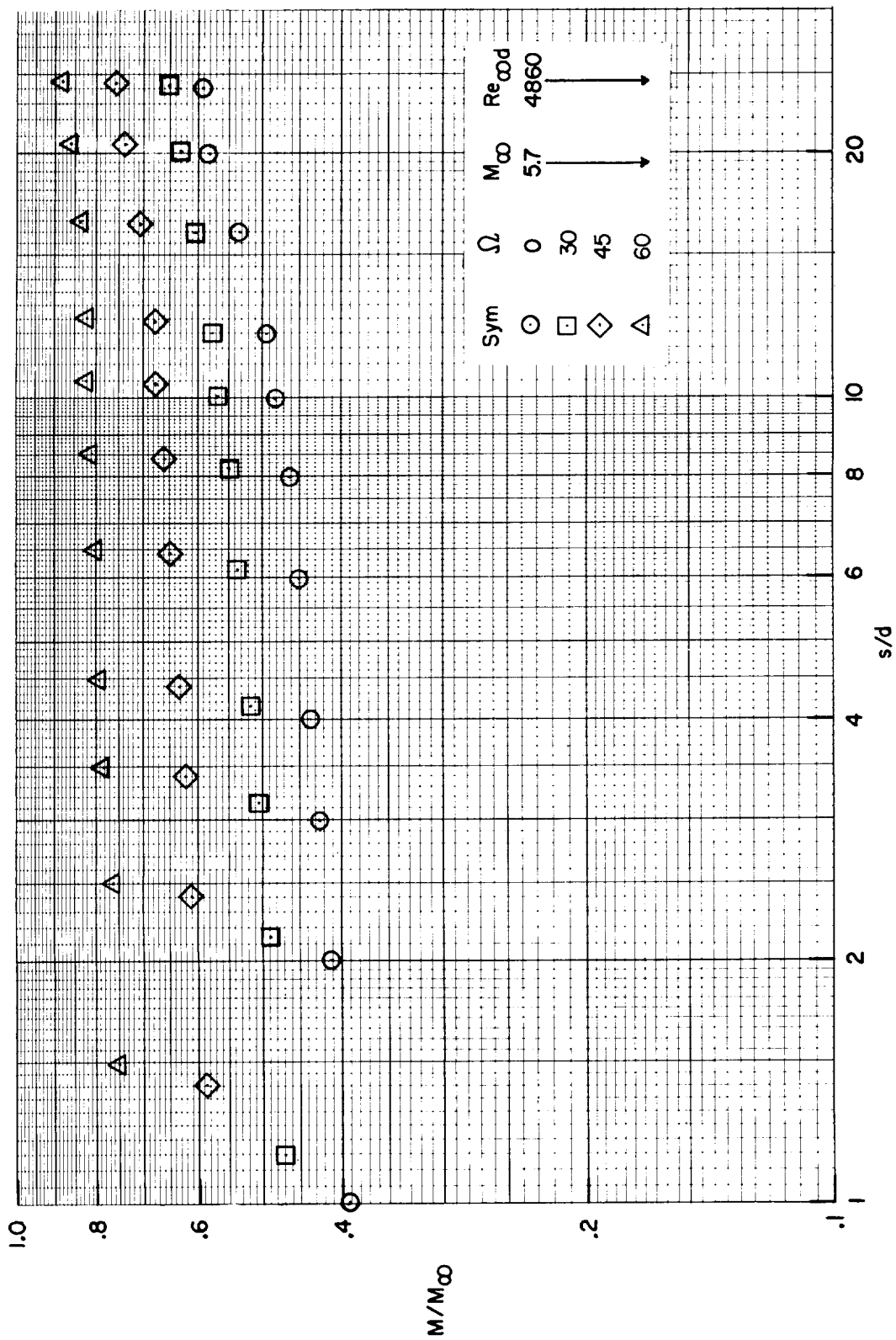


Figure 17.- Variation of the ratio of local to free-stream Mach number with streamwise distance from the swept leading edge of blunt plates.

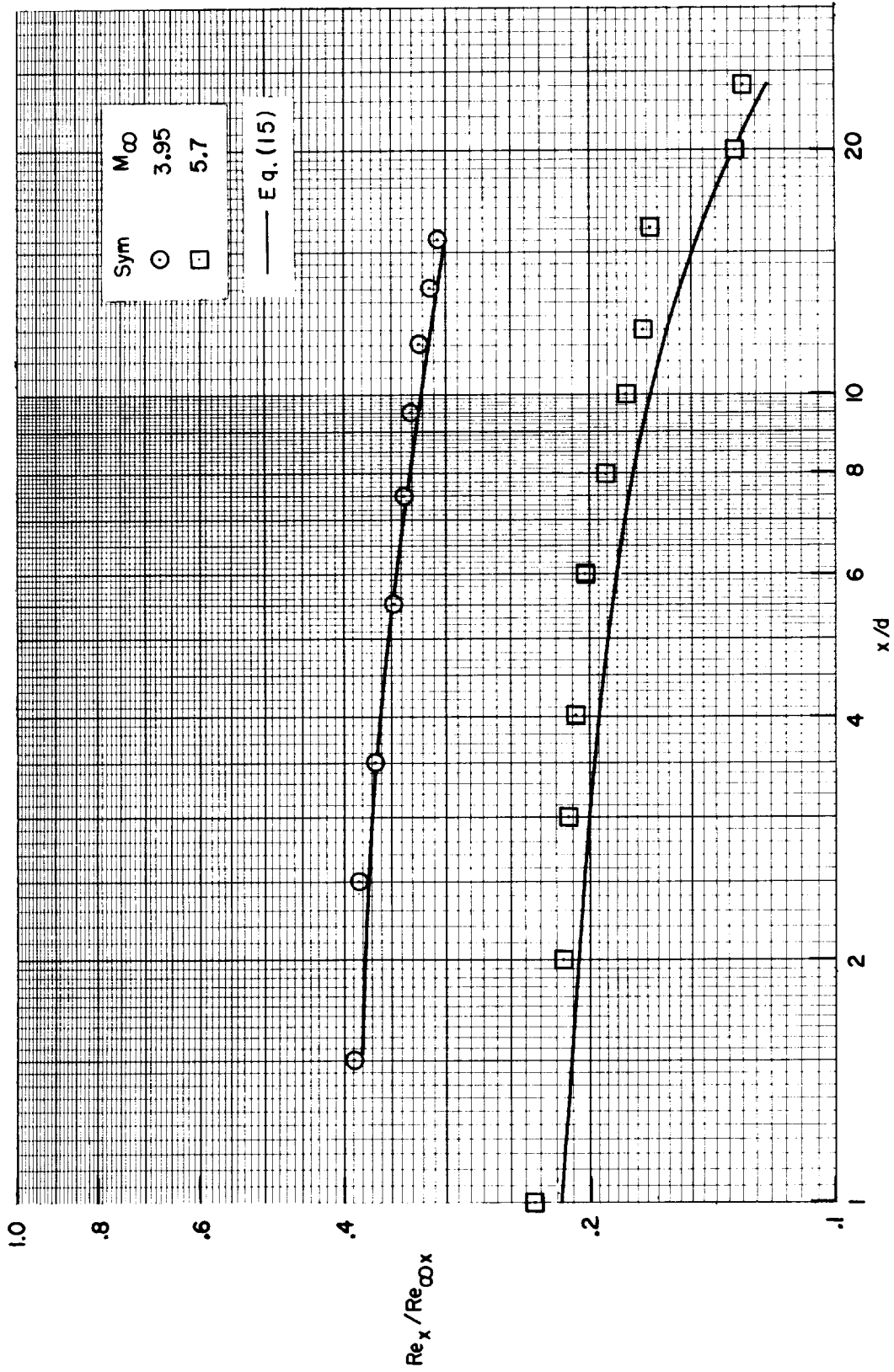


Figure 18.- Effect of the free-stream Mach number on the local Reynolds number along the boundary-layer edge; $\Omega = 0$, $\alpha = 0$.

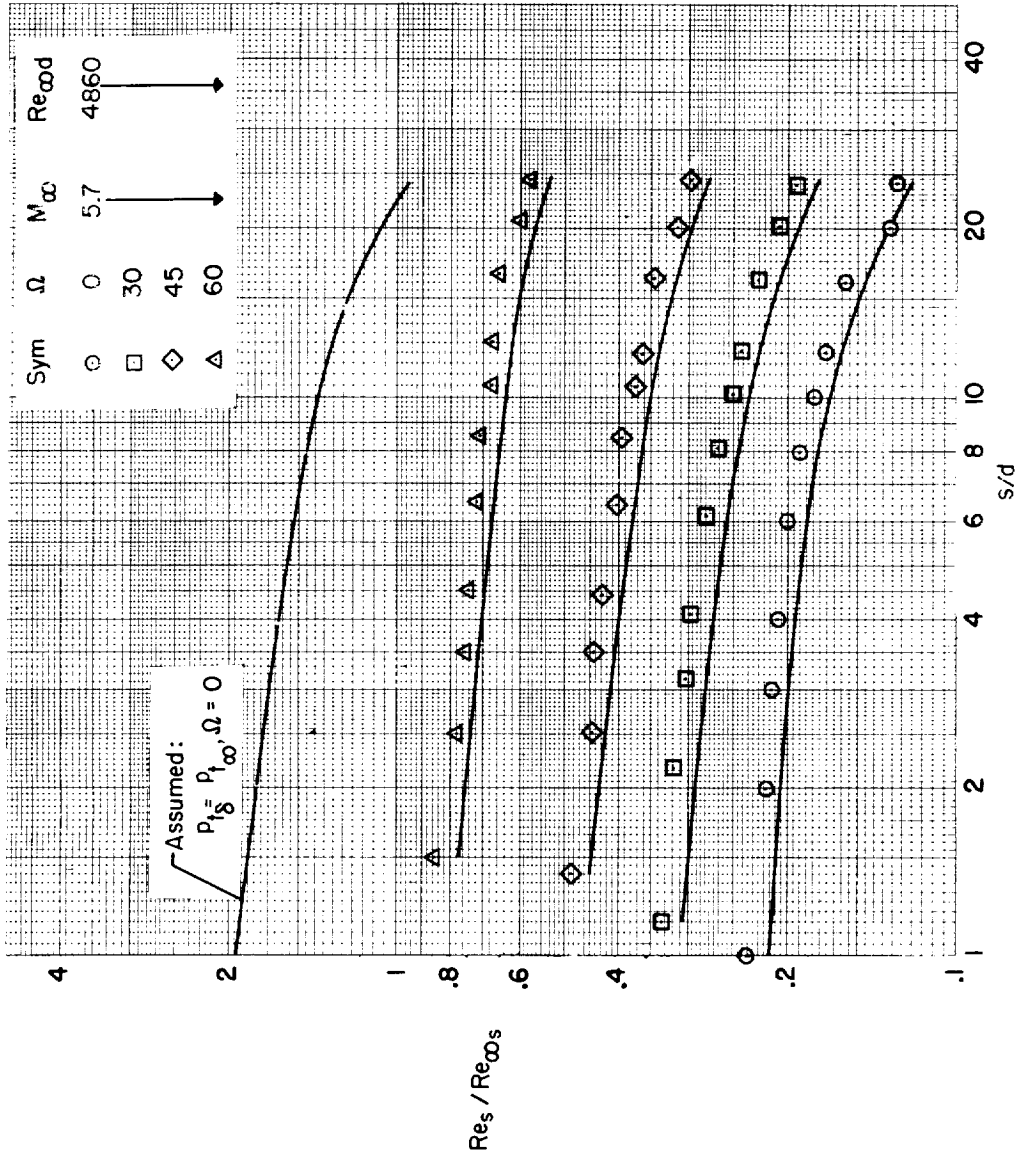


Figure 19.- Comparison of measured variation of local Reynolds number with that predicted by equation (15).

NASA MEMO 12-26-58A
National Aeronautics and Space Administration.
THE EFFECT OF LEADING-EDGE SWEEP AND
SURFACE INCLINATION ON THE HYPERSONIC
FLOW FIELD OVER A BLUNT FLAT PLATE.
Marcus O. Creager. January 1959. 45p. diags.,
photo., tabs. (NASA MEMORANDUM 12-26-58A)

Surface pressures were measured on blunt flat plates
with various values of angle of attack and of leading-
edge sweep for Mach numbers of 4 and 5.7 and
Reynolds numbers per inch of 6,600 and 20,000. Sur-
face pressures were correlated for a wide range of
variables by a method developed from boundary-layer
and blast-wave theory. Boundary-layer thicknesses
and shock-wave locations were determined from flow-
field surveys. A method was developed to predict the
variation in local Reynolds number with leading-edge
sweep.

Copies obtainable from NASA, Washington

1. Flow, Supersonic
(1.1.2.3)
 2. Flow of Rarefied Gases
(1.1.5)
 3. Boundary Layer - Wing
Section (1.2.1.6)
 4. Wings, Complete -
Sweep (1.2.2.2.3)
- I. Creager, Marcus O.
II. NASA MEMO 12-26-58A

NASA

NASA MEMO 12-26-58A
National Aeronautics and Space Administration.
THE EFFECT OF LEADING-EDGE SWEEP AND
SURFACE INCLINATION ON THE HYPERSONIC
FLOW FIELD OVER A BLUNT FLAT PLATE.
Marcus O. Creager. January 1959. 45p. diags.,
photo., tabs. (NASA MEMORANDUM 12-26-58A)

Surface pressures were measured on blunt flat plates
with various values of angle of attack and of leading-
edge sweep for Mach numbers of 4 and 5.7 and
Reynolds numbers per inch of 6,600 and 20,000. Sur-
face pressures were correlated for a wide range of
variables by a method developed from boundary-layer
and blast-wave theory. Boundary-layer thicknesses
and shock-wave locations were determined from flow-
field surveys. A method was developed to predict the
variation in local Reynolds number with leading-edge
sweep.

Copies obtainable from NASA, Washington

1. Flow, Supersonic
(1.1.2.3)
 2. Flow of Rarefied Gases
(1.1.5)
 3. Boundary Layer - Wing
Section (1.2.1.6)
 4. Wings, Complete -
Sweep (1.2.2.2.3)
- I. Creager, Marcus O.
II. NASA MEMO 12-26-58A

NASA

NASA MEMO 12-26-58A
National Aeronautics and Space Administration.
THE EFFECT OF LEADING-EDGE SWEEP AND
SURFACE INCLINATION ON THE HYPERSONIC
FLOW FIELD OVER A BLUNT FLAT PLATE.
Marcus O. Creager. January 1959. 45p. diags.,
photo., tabs. (NASA MEMORANDUM 12-26-58A)

Surface pressures were measured on blunt flat plates
with various values of angle of attack and of leading-
edge sweep for Mach numbers of 4 and 5.7 and
Reynolds numbers per inch of 6,600 and 20,000. Sur-
face pressures were correlated for a wide range of
variables by a method developed from boundary-layer
and blast-wave theory. Boundary-layer thicknesses
and shock-wave locations were determined from flow-
field surveys. A method was developed to predict the
variation in local Reynolds number with leading-edge
sweep.

Copies obtainable from NASA, Washington

1. Flow, Supersonic
(1.1.2.3)
 2. Flow of Rarefied Gases
(1.1.5)
 3. Boundary Layer - Wing
Section (1.2.1.6)
 4. Wings, Complete -
Sweep (1.2.2.2.3)
- I. Creager, Marcus O.
II. NASA MEMO 12-26-58A

NASA

1. Flow, Supersonic
(1.1.2.3)
 2. Flow of Rarefied Gases
(1.1.5)
 3. Boundary Layer - Wing
Section (1.2.1.6)
 4. Wings, Complete -
Sweep (1.2.2.2.3)
- I. Creager, Marcus O.
II. NASA MEMO 12-26-58A

NASA

